Nano Today 26 (2019) 108–122

Contents lists available at ScienceDirect

Nano Today

journal homepage: www.elsevier.com/locate/nanotoday

Review

Inherent multifunctional inorganic nanomaterials for imaging-guided cancer therapy

Yanmin Ju[a,b], Bing Dong[a], Jing Yu[c], Yanglong Hou[a,*]

[a] Beijing Key Laboratory for Magnetoelectric Materials and Devices, Department of Materials Science and Engineering, College of Engineering, Peking University, Beijing Innovation Centre for Engineering Science and Advanced Technology, Beijing, 100871, China
[b] College of Life Science, Peking University, Beijing, 100871, China
[c] Research Center of Magnetic and Electronic Materials, College of Materials Science and Engineering, Zhejiang University of Technology, Hangzhou, 310014, China

ARTICLE INFO

Article history:
Received 22 December 2018
Received in revised form 20 February 2019
Accepted 18 March 2019
Available online 29 March 2019

Keywords:
Inherent function
Inorganic nanomaterials
Imaging techniques
Cancer therapy

ABSTRACT

Nanomaterials offer tremendous potential for cancer imaging and therapy due to their unique intrinsic characteristics. Combining imaging and therapeutic agents in one nanoplatform can bring great benefits for simultaneous diagnosis and therapy. However, incorporating different functional moieties together to form multifunctional nanoplatform increase the steps of synthesis and difficulties of purification, which is hard for reproducibility, scale-up and further toxicity study. Thus, engineering nanomaterials with components that possesses multiple intrinsic functionalities as both imaging and therapy agents, which mostly are derived from inorganic materials, would simplify the composition of nanomaterials to get uniform nanostructures. In this review, we will focus on the recent reports on the multifunctional inorganic nanoplatforms built from the components possessing multiple intrinsic functionalities, which can be applied in imaging-guided therapy, including magnetic hyperthermia, photothermal therapy, photodynamic therapy, chemodynamic therapy, surgery and synergistic therapy.

Contents

* Corresponding author at: Peking University, Beijing, 100871, China.
E-mail address: hou@pku.edu.cn (Y. Hou).

https://doi.org/10.1016/j.nantod.2019.03.006
1748-0132/

Introduction

Cancer is one of leading causes of death in the world and many efforts from different research fields have been made to explore the strategies to cure the cancer with high efficiency and low toxicity [1]. Nanomaterials (including liposomes, metallic particles, polymers, micelles etc.) have drawn a great deal of interest in cancer treatment due to their various exciting possibilities in cancer diagnose and therapy.

Because of the large surface area or interior empty volume, nanomaterials can serve as carriers to delivery large amount of drugs through chemical conjugation or loading, which could solve the problems of free drugs, including poor stability and solubility, rapid metabolism and clearance, and uptake unselectively by healthy cells. Progress has been made when using several nanoparticles (NPs) as drug carriers currently approved in preclinical and clinical trial [2,3]. Besides, nanomaterials relying on their intrinsic properties can be triggered by external stimuli and utilized in therapy. External stimuli, such as light [4], magnetic field [5,6], radiation [7], ultrasound [8], and temperature [9], have also been exploited to trigger nanomaterials, which has the advantages of spatial and temporal control for applications such as photodynamic therapy [10], hyperthermal therapy [11], radiotherapy [12], or drug delivery and release [13]. Such as radio-induced tumor cell killing of hafnium oxide NPs have been demonstrated in mouse models during Phase 1 clinical trial [14].

Except the external stimuli, the properties of tumor microenvironment are unique from normal tissues, which also can be considered to engineer nanomaterials. Tumor blood vessels have leaky vasculature and poor lymphatic drainage compared with normal parts, which is known as the enhanced permeability and retention (EPR) effect [15]. Nanomaterials with small sizes between 10–200 nm can show increasing accumulation in tumor sites, which is called as passive targeting [16]. However, passive targeting doesn't work in all types of tumors. Therefore, active targeting, by conjugating biological markers (e.g. folate [17], RGD [18], transferrin [19]) to the surface of NPs, can make sure NPs enter into specific tumor cells that overexpress specific receptors more efficiently. Besides, the pH value of tumor environment is lower and the reduction potential is different. Enzymes like matrix metalloproteinase are overexpressed in the environment of tumors [20]. These internal properties can trigger functional nanomaterials to release drugs or improve the tumor cell internalization of nanomaterials specifically.

When nano-system enter into the changeable and complicated tumor microenvironment, imaging techniques could be helpful for visualization of the treatment process. During the development of biological imaging techniques, imaging probe or contrast agent is introduced to improve its sensitivity and detectability in the image visibility. Without the contrast agent, images would be limited and unable to provide such rich information [21]. Fortunately, there are some nanomaterials can act as both therapeutic agents and imaging contrast agents, which means they can achieve imaging-guided cancer therapy, which enables to visualize the size and location of tumors before therapy and evaluate the treatment efficiency during and after therapy. Imaging modalities such as magnetic resonance imaging (MRI), X-ray computed tomography (CT), positron emission tomography (PET) and ultrasound are utilized for clinical diagnosis nowadays. Compared to small molecule imaging agents or drugs, nanomaterials can integrate two or more kinds of imaging and therapy agents together, which can overcome the limitation of each imaging technique and get more integral information and synergetic therapeutic effect in clinic.

There are two different approaches to achieving nanoplatforms with multifunctional abilities for imaging-guided therapy. One is combining functional moieties (drugs, imaging agents, etc.) into the one single nanoparticle together through encapsulating or conjugating or absorbing the agent to others, while the other is utilizing components with inherent functionalities as imaging and therapy agents, which mostly are derived from inorganic materials, to build inherent multifunctional nanomaterials. In this review, we will focus on the latter approach and propose the concept of inherent inorganic nanomaterial engineering for imaging-guided cancer therapy. We will summary intrinsic functional inorganic components which can be applied for cancer imaging and therapy. Besides, we will focus on the recent reports on the inherent multifunctional inorganic nanoplatforms and their applications in imaging-guided therapy, including magnetic hyperthermia, photothermal therapy, photodynamic therapy, chemodynamic therapy and surgery. The development of intrinsically multifunctional inorganic nanomaterials may open the era of cancer diagnosis and therapy in clinic in the future.

The concept of inherent inorganic nanomaterial engineering

Multifunctional nanoplatform for biomedical imaging and therapy should have various functional properties including imaging agents, therapeutic agents (drugs, proteins and genes), targeting molecule or external/internal triggered agents [22,23]. These functionalities should be incorporated into the one single nanoparticle during the engineering of nanomaterials relying on the careful design plan, which could ensure nanoplatform for imaging and therapy theoretically.

There are two approaches for accomplishing the above target. One is combining functional moieties (drug, imaging agents, etc.) into the one single nanoparticle together through encapsulating or conjugating or absorbing the agent to others. Since the available moieties and multiple combination methods (encapsulating, conjugating, adsorbing and so on), it could be convenient and efficient to achieve new nanomaterials. So various multifunctional nanoparticle have been reported following this approach. However, with the increasing complexity of the design of nanomaterials, it could be more and more difficult to accomplish the target since the steps of synthesis and purification should be increased, which means hard for reproducibility and scaling-up. Besides, it is complicated for toxicity studies as multiple moieties and the difficult to guarantee uniformity of each nanoparticle.

The other approach is using components with inherent functionalities as imaging and therapy agents to build inherent multifunctional nanomaterials. The advantages of this approach include: (1) decrease the difficulty of the design and simplify the composition of the multifunctional nanomaterials while maintaining the desired properties and following the principles of green chemistry, (2) monitor the location of the nanomaterials and the therapy process rely on imaging techniques since different functional components are merged together in each nanoparticle and have no separation problem, (3) have high-usage of the chemicals and possess lower clinical translation hurdles because NPs are uniform and have all functional components from the reaction system, which means much easier toxicity studies.

Therefore, the materials that possess intrinsically multifunctional capabilities are urgently needed to be exploited as the building blocks for the design. The intrinsic materials are categorized into organic and inorganic. Organic NPs including dendrimers, polymeric micelles and liposomes are conventionally used as carriers and delivery systems [24–31]. In this manuscript, we will focus on inorganic nanomaterials with intrinsic imaging and/or therapeutic properties, such as iron oxide NPs for MRI and thermal therapy [32,33], gold nanomaterials for CT, radiation therapy and photothermal therapy [34–36], carbon-based NPs [37,38],

Table 1
Intrinsic functions of inorganic nanomaterials for imaging and therapy.

Modality	Component	References
MRI	Paramagnetic transition and lanthanide metal ions (Fe^{3+}, Mn^{2+}, Cu^{2+}, Gd^{3+})	[42]
	NPs of paramagnetic ions (Gd_2O_3, GdF_3, $GdPO_4$, MnO)	[43,44,45,46]
	Superparamagnetic nanoparticle (Fe_3O_4, $MnFe_2O_4$, $CoFe_2O_4$, $NiFe_2O_4$)	[21]
CT	Iodine	[47]
	Gold	[48]
	Bismuth	[49]
	Tantalum	[50]
Optical imaging	Quantum dots	[51]
	Lanthanide atom	[52]
	Carbon nanotube	[53]
	Gold-based nanostructures	[54]
PET, SPECT	^{18}F, ^{11}C, ^{89}Zr, ^{64}Cu, ^{68}Ga, ^{86}Y	[55]
	^{99m}Tc, ^{111}In, ^{67}Ga, ^{123}I, ^{125}I, ^{131}I	[56]
PAI	Metal and semiconductor materials (Ag, Au, carbon, quantum dots)	[57,58]
Hyperthermia	Magnetic NPs	[59,60,61]
PTT	Noble metal-based nanomaterials (Au, Cu, Pd)	[62,63]
	Carbon nanotube	[64]
	Graphene	[51]
	Transitional metal compounds (MoS_2, WS_2, Bi_2Se_3)	[65]
PDT	Quantum dots	[66,67]
	Graphene carbon	[68]
CDT	Iron-based nanomaterials	[69,70,71,72,73]
	Other metal-based nanomaterials (Mn^{2+}, Co^{2+}, Cu^{2+})	[74,75,76]
Surgery	Fluorescent dye	[77,78,79]
	Gold-based nanomaterials	[80]

MRI: magnetic resonance imaging; CT: X-ray computed tomography; PET: positron emission tomography; SPECT: single photon emission computed tomography; PAI: photoacoustic imaging. PTT: photothermal therapy; PDT: photodynamic therapy; CDT: chemodynamic therapy.

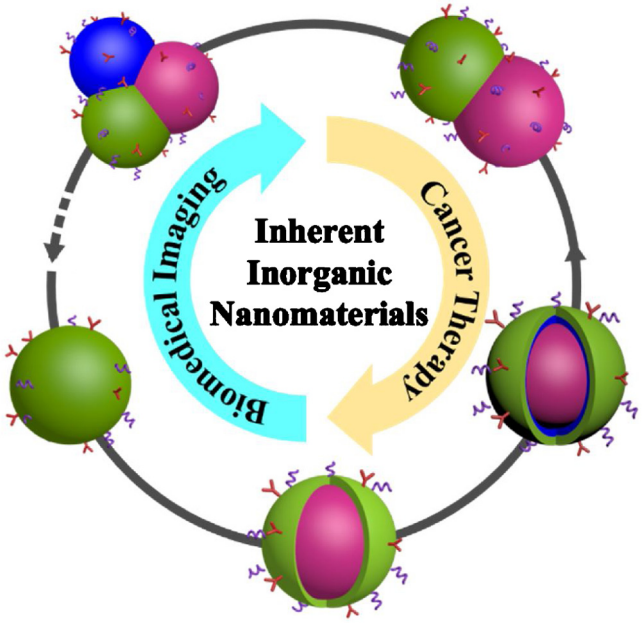

Fig. 1. Schematic representation of the concept of inherent inorganic nanomaterial engineering. The nanomaterials built from the inorganic components with multiple intrinsic functionalities (single block, core@shell heterostructure, dimer heterostructure, and triple heterostructures) could achieve reproducibility and scale-up easier than nanomaterials combining different functional moieties (drug, imaging, etc.) together into one single nanoparticle.

bismuth-containing nanomaterials for CT, photoacoustic (PA) and photothermal therapy [39], copper chalcogenides-based nanomaterials for MRI, near infrared imaging and photothermal therapy [40], quantum dots (QDs) for photodynamic and radiation therapy [7,41]. Table 1 summarizes inorganic components with intrinsic imaging and therapeutic properties, which could be the guide for synthesizing multifunctional inorganic nanomaterials.

As shown in Fig. 1, according to the morphology and component of the inherent nanomaterials, they could be divided into monocomponent single block, core@shell heterostructure, dimer heterostructure, and multicomponent heterostructure. The multicomponent hybrid nanoparticle often possess different surface properties, crystal lattices, redox potentials or surface charge, so successful combination of intrinsic multifunctional components into a hybrid nanoparticle still need to achieve suitable synthetic methods [81,82].

Seed-mediated growth is the most common method to obtain multicomponent hybrid nanoparticle through sequential nucleation and growth of a second or more components on the performed seeds. To achieve the hybrid nanoparticle nucleation, the lattice spacing between two components should be well-matched. The charge transfer between the seeds and newly nucleated components should also be considered since they will change the energy for heterogeneous nucleation. Meanwhile, seed-to-precursor ratio, reactant concentration and heating profile should be regulated to ensure the formation of multicomponent heterostructures [83]. These inorganic nanomaterials should be able to disperse in water and keep stability, which is the first step for their further biomedical application. They could be modificated by polymer (polyvinyl acetate (PVA), polyethylene glycol (PEG), chitosan), inorganic materials (silicon dioxide, gold), and small molecule which could have strong coordination capability of group with NPs [84].

For example, Sun's group achieved Fe_3O_4@Au NPs by reducing $HAuCl_4$ to form Au and further coating on the surface of Fe_3O_4 NPs in oleylamine. And Fe_3O_4@Au NPs in an organic environment could be transferred into water with cetrimonium bromide (CTAB) [85]. Our group synthesized Janus-like Au-Fe_2C heterostructures by reducing $Fe(CO)_5$ on the seed of Au to form Au-Fe heterostructures, which were further carbonized in octadecene to get Au-Fe_2C heterostructures. The heterostructures were modificated by 1,2-distearoyl-snglycero-3-phosphoethanolamine-N-[amino(polyethylene glycol)-2000] (DSPE-PEG-NH_2) and showed excellent biomedical stability in phosphate-buffered saline (PBS) solution, cell culture medium, and cell culture medium with 10% fetal bovine serum (FBS) [86].

Following the design plan, suitable components could be the candidate to synthesize heterostructures. For example, we synthe-

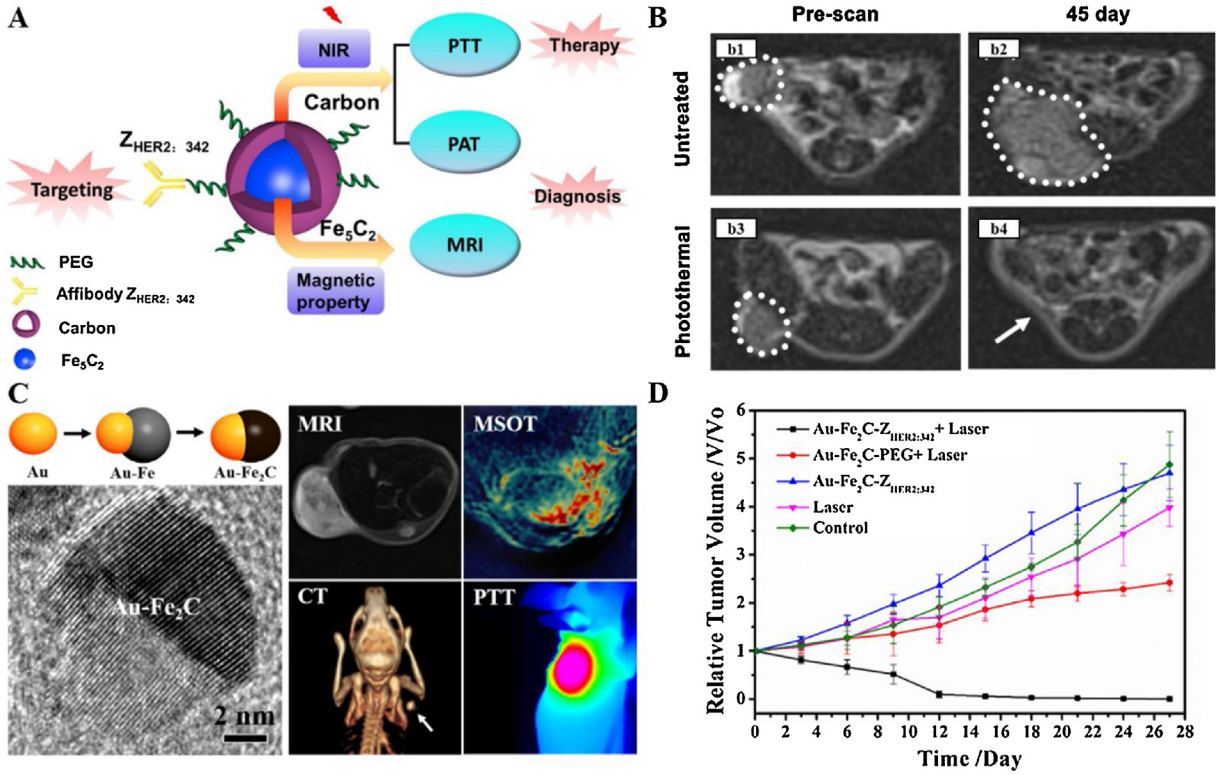

Fig. 2. (A) Scheme for the design of Fe_5C_2 NPs as photoacoustic tomography and magnetic resonance imaging-guided phototherapy agents. (B) T_2 MR images of mice: (b1), (b2): mouse was injected with Fe_5C_2-$Z_{HER2:342}$ only, and, (b3), (b4) mouse was injected with Fe_5C_2-ZHER$_{2:342}$ and irradiated under 808 nm at the tumor sites after intravenous injection. Reproduced with permission from ref. [87]. Copyright © 2014, Wiley-VCH Verlag GmbH & Co. KGaA, Weinheim. (C) Scheme for the design of Au-Fe_2C NPs as photoacoustic tomography/magnetic resonance imaging/computed tomography-guided phototherapy agents. (D) Tumor growth curves of mice from the five different treatment groups, which were normalized to the initial sizes. Reprinted with permission from ref. [86]. Copyright © 2017, American Chemical Society.

sized iron carbide NPs and found they had the potential as agents for MRI/PA-guided photothermal therapy with no systematic side effects [87]. Based on this exciting results, we tried to further optimize their performance as triple-modal imaging agents with high photothermal transduction efficiency. We chose optical classical material Au as the seed and got monodispersed Au-Fe_2C janus NPs, which can both provide more accurate information for diagnosis and ablate tumors for therapy. And we studied the toxicity of Au-Fe_2C easily owing to their homogenous structures (Fig. 2) [86]. However, we cannot choose and combine functional components randomly to obtain multicomponent inherent NPs since many factors influence the synthesis process as we mentioned above.

Conventional imaging techniques

Nowadays, there are broadly two categories of imaging modalities in clinic: primarily anatomical imaging techniques with high spatial resolution, MRI, CT and ultrasound (US) imaging, the others are primarily molecular imaging techniques, which can detect molecular and cellular changes of tissues, including nuclear imaging (positron emission tomography (PET) and single photon emission computed tomography (SPECT)), optical imaging [88]. In clinical detection and treatment, all these imaging modalities are irreplaceable accessories for doctors because they have different characteristics and suitable for different tissues considering parameters like sensitivity and depth/spatial resolution [89]. The characteristics of different imaging techniques and corresponding contrast agents made form nanomaterials will be introduced in this parts. And characteristics of different imaging techniques are also listed in Table 2.

Magnetic resonance imaging

MRI, a non-invasive imaging technique, is time-consuming and expensive in clinic. But it can offer high resolution and deep tissue penetration to visualize anatomical details of soft tissue [21,90,91,100]. The basic principle of MRI is based on nuclear magnetic resonance (NMR) technology and relaxation of the nuclei of proton spins in a strong magnetic field. When exposed to a strong magnetic field, nuclei of proton spins align parallel or antiparallel to the field and precess under a frequency named as Larmor frequency (Fig. 3A). The protons absorb energy and are excited to higher-energy state when the radio-frequency (RF) is introduced to the system. With the disappearance of the RF pulse, the active nuclei relax immediately back to their initial state. There are two kinds of relaxation processes, which can both be utilized in generating MR images to distinguish different types of tissue. One is longitudinal or T_1 relaxation that involves the decreased net magnetization (M_z) recovering to the initial state, which is bright in images. The other called transverse or T_2 relaxation that refers to the induced magnetization on the perpendicular plane (M_{xy}) disappearing, which is dark in images (Fig. 3B).

Relying on the above relaxation pathways, the contrast agents are also classified into T_1 and T_2 contrast agents to differentiate signal and parameter from MR images in different tissues. The former type is mainly paramagnetic transition and lanthanide metal ions complexes with many unpaired electrons, such as Gd^{3+}, Mn^{2+}, Cu^{2+} and Fe^{3+}. So NPs with compounds of transition and lanthanide metals could be excellent candidates for T_1 MRI contrast agents because of the metal ions with high magnetic moments on their surface [42]. Such as Gd_2O_3 [43], GdF_3 [44] and $GdPO_4$ [45] and MnO NPs [46]. The latter type is based on paramagnetic or superparamagnetic iron

Table 2
Characteristics of different imaging techniques.

Imaging technique	Advantages	Disadvantages	Reference
MRI	High spatial resolution; Providing physiological and molecular information; No limited tissue penetration.	Low sensitivity; Long-time imaging; Expensive cost.	[90,91]
CT	High spatial resolution; No limited tissue penetration;	Exposed to radiation; Hard to distinguishing soft tissues.	[92]
Fluorescent imaging	High sensitivity High temporal resolution; Easy to discrimination.	Limited tissue penetration; Low spatial resolution.	[93,94,95]
PET	High sensitivity; No limited tissue penetration; Suitable for whole body.	Exposed to radiation; Expensive cost.	[96]
SPECT	High sensitivity; No limited tissue penetration.	Exposed to radiation; Limited spatial resolution.	[96,97]
PAT	Higher penetration depth and spatial resolution; High sensitivity; Providing molecular and functional information.	Limited in imaging agents.	[98,99]

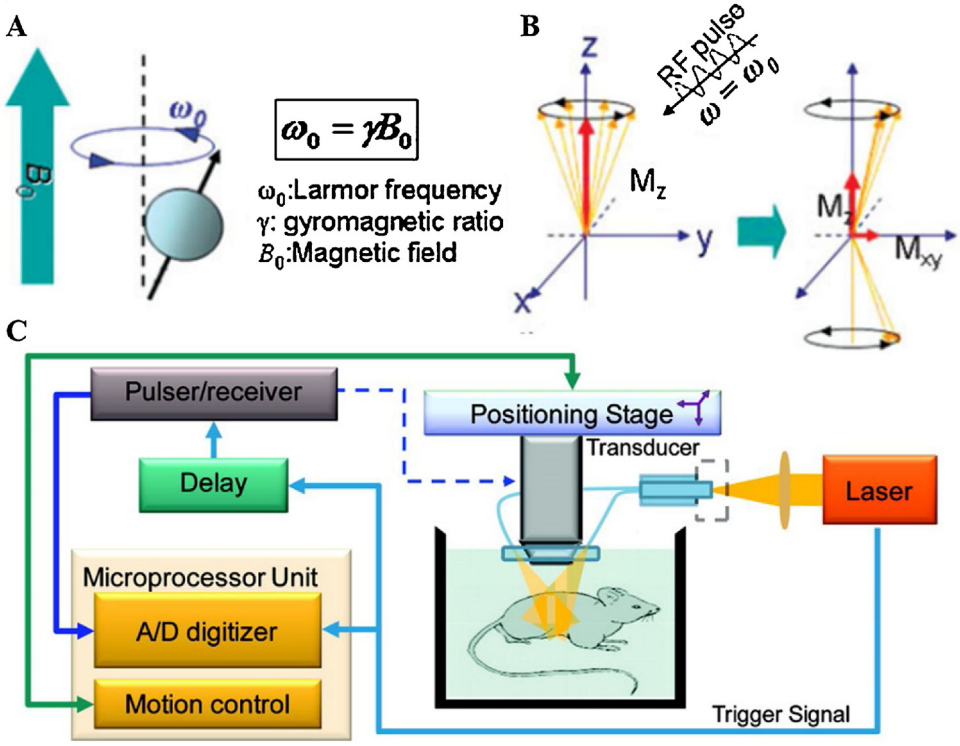

Fig. 3. Principle of magnetic resonance imaging. (A) Spins align parallel or antiparallel to the field and precess under Larmor frequency (ϖ_0). (B) After induction of radio-frequency (RF) pulse, magnetization of spins changes. Reproduced with permission from ref. [21]. Copyright © 2019, WILEY-VCH Verlag GmbH & Co. KGaA. (C) Block diagram of a typical photoacoustic imaging system. Reproduced with permission from ref. [100]. Copyright © 2009, American Chemical Society.

oxide NPs with strong magnetization when applied in an external magnetic field. Interestingly, iron oxide NPs can be both T_1 and T_2 MRI contrast agents by regulating their sizes [21,101]. Ultrasmall superparamagnetic iron oxide NPs with sizes (< 6 nm) were found to be good candidates for T_1-weighted MRI [102]. There are several commercial MRI contrast agents based on iron oxide NPs, such as such as Feridex, Resovist, and Combidex [103]. And alloy materials, like $CoFe_2O_4$, $MnFe_2O_4$, and $NiFe_2O_4$, also can be candidates as T_2 contrast agents [21].

Computed tomography

CT, one of the leading radiology technologies, is the most convenient imaging tools used in clinic today considering cost, availability and efficiency. CT can visualize bone structures clearly because of the innate contrast between the more permeable soft tissues and electron-dense bones. However, CT is limited in distinguishing different soft tissues with similar densities because the mechanism of CT to distinguish different tissues is based on different degrees of X-ray attenuation of various tissues [92].

In order to provide better contrast in CT images and better depiction of soft tissue structures with similar contrast properties, CT contrast agents are urgently needed in CT techniques. The key factor in selecting CT contrast agents is high atomic number materials. Conventional and present clinical CT contrast agents are based on the high atomic number iodine-based molecules, which are effective in absorbing X-rays but rapid cleared by the kidneys. Larger size of iodine-based contrast agents can address this limitation [47]. Except that, metal NPs such as gold [48], bismuth [49] and tantalum [50], can produce contrast higher than iodine-based agents, which means they have a great potential in CT imaging.

Optical imaging

Optical imaging is an imaging technique relying on the behavior and properties of ultraviolet, visible and infrared light. Optical imaging techniques include bioluminescence imaging, chemiluminescence imaging, optical coherence tomography (OCT), surface enhanced Raman scattering-based imaging, afterglow imaging and fluorescence imaging [104–109]. Among them, fluorescence imaging is the most widely used in clinic, which is based on the absorption and emission of energy from external light through fluorophores. Near-infrared (NIR) light, ranging from 700 nm to 1100 nm, is minimally absorbed and penetrate deeper than visible light in biological tissues. To overcome the photon attenuation and low penetration caused by the visible region, fluorescent probes with long emission at the NIR region have been developed rapidly. The number of NIR probes continues to grow owing to the progress in nanomaterials, such as QDs made from semiconductor NPs possessing optical property [51], various optically active lanthanide ions [52], carbon nanotube with tunable near-infrared emission [53] and gold-based nanostructures with localized surface plasmon resonance (LSPR) [54]. Remarkably, fluorescence imaging in the second near-infrared window (NIR-II, wavelength 900–1400 nm) is more desirable than NIR-I imaging (700–900 nm) because of deeper tissue penetration, reduced photon scattering and lower autofluorescence. The potential NIR-II fluorescence imaging agents includes carbon nanotubes [93,94], certain types of QDs [95] and several small-molecule dyes [110].

PET and SPECT imaging

PET and SPECT are imaging methods based on nuclear magnetic resonance (NMR) technology. Despite that both of them can image and quantify the *in vivo* distribution of positron-emitting radioisotopes injected into the body, they still have some differences. Firstly, PET has better image resolution and higher precision than SPECT and already is widely used in clinical assessment of tumor. PET offers a resolution of 5–7 mm in cardiac tissues while a SPECT resolution can only achieve 12–15 mm [111]. So PET can identify biological and anatomical structure which might be hidden by SPECT. Secondly, SPECT can use compounds with two or more radioisotopes to label the biological structure [96,97]. Meanwhile, SPECT is much lower-cost than PET in clinical applications.

Common PET radionuclides include ^{18}F, ^{11}C, ^{89}Zr, ^{64}Cu, ^{68}Ga, and ^{86}Y, [55] and common radionuclides used in SPECT include ^{99m}Tc, ^{111}In, ^{67}Ga, ^{123}I, ^{125}I, and ^{131}I [56]. The difference between radionuclides of PET and SPECT is half-life of the isotope that each technique uses. SPECT radionuclides have a relatively long half-life while short half-life is a limitation of the current PET ones. These isotopes all need to chelate with compounds, such as ^{11}C-raclopride [112], ^{18}F-FDDNP [113], ^{64}Cu-DOPA [114], ^{99m}Tc-sestamibi [115]. Recently, researchers use nanocarriers to handle nuclear isotopes in the biological environment [116].

Photoacoustic imaging

Photoacoustic imaging is a hybrid biomedical imaging modality, which combines the high contrast of optical imaging and the high spatial resolution of ultrasound imaging together. Photoacoustic imaging is based on the photoacoustic effect, which can induce tissue heating due to the absorption of non-ionizing laser pulses by biological tissues or exogenous contrast agents and subsequently produce wideband acoustic waves at megahertz frequencies because of transient thermoelastic expansion [98]. These photoacoustic waves can be detected by ultrasound transducers at the tissue surface and reconstructed to form ultrasound images (Fig. 3C). Photoacoustic imaging has already been proved as a powerful technique for visualizing biological structures with contrast, penetration depth and spatial resolution, overcoming the limitations of optical imaging or ultrasound imaging only [99].

Exogenous contrast agents can used to enhance photoacoustic imaging except the improvement of instrument. One of the most important factors to design the contrast agents is to assess the ability of converting absorbed light to ultrasound waves. Metal and semiconductor materials possess this function, such as silver, gold, carbon, and QD [57,58]. These structures have great potential in photoacoustic imaging for distinguishing diseased tissue from healthy tissue by reconstructing the composition, shape, and size.

Imaging-guided cancer therapy

Some nanosystems for delivering therapeutic agents rely on their own special functions including external stimuli and internal tumor characteristics, which could not ensure nanosystem target to tumor sites with high efficiency owing to cancers are heterogeneous and all cancer treatments are only effective for limited cancer types or even at selective cancer stages. Imaging-guided therapy could provide precise disease information as they can visualize the size and location of tumors before therapy and evaluate the treatment efficiency during and after therapy, which means more likely to provide improved prognoses. Here, we will mainly focus on intrinsically multifunctional inorganic nanoplatform with capabilities as therapeutic methods with imaging guidance, including magnetic hyperthermia, photothermal therapy, photodynamic therapy, chemodynamic therapy, surgery and synergistic therapy.

Imaging-guided magnetic hyperthermia

Hyperthermia is a kind of cancer treatment which change the physiology of tumor cells directly and lead to apoptosis finally by exposing tumor sites to high temperatures. Hyperthermia treatment could be divided into three types according to the increased temperature, including diathermia (<41 °C), moderate hyperthermia (41 °C < T <46 °C), thermo ablation (> 46 °C). Traditional hyperthermia treatment actually is moderate hyperthermia, which can cure cancer by prompting the immune system or inducing cell death directly by either necrosis or apoptosis, while the normal cells could survive [117]. Hyperthermia treatment heated the whole body is only suitable for treating metastatic cancer that spread over the whole body. Otherwise, the healthy tissues would also be harmed for the long time heating. External devices such as ultrasound, and microwaves that can transfer other energy into thermal energy was applied in the treatment, but they still had a serious threat to the normal tissues. Until Gilchrist et al. first found the heating phenomenon by using γ-Fe_2O_3 NPs converting magnetic energy into thermal energy when exposed to an external magnetic field [59]. After that, magnetic NPs have been widely used for hyperthermia, which has been a hotspot to cure cancer because of advantages of localized heating controlled by external magnetic field. Magnetic iron oxide-based hyperthermia passed the preclinical stage and were studied in humans after direct injection of nanoparticles into solid tumors treatment [60,61].

Hysteresis and relaxation behavior are considered as two major factors that explain the reason of heat generated by magnetic NPs under an alternating magnetic field. Hysteresis causes from the internal energy of magnetic NPs and is the main mechanism for ferromagnetic NP-based hyperthermia. Relaxation behavior, including Brown and Néel relaxation way, is suitable for the explanation of superparamagnetic NPs. Brownian relaxation means the rotation of the particles while Néel relaxation refers to the rotation of the moment within each particles. The relaxation process is controlled by the faster one. However, when NPs enter into intra-

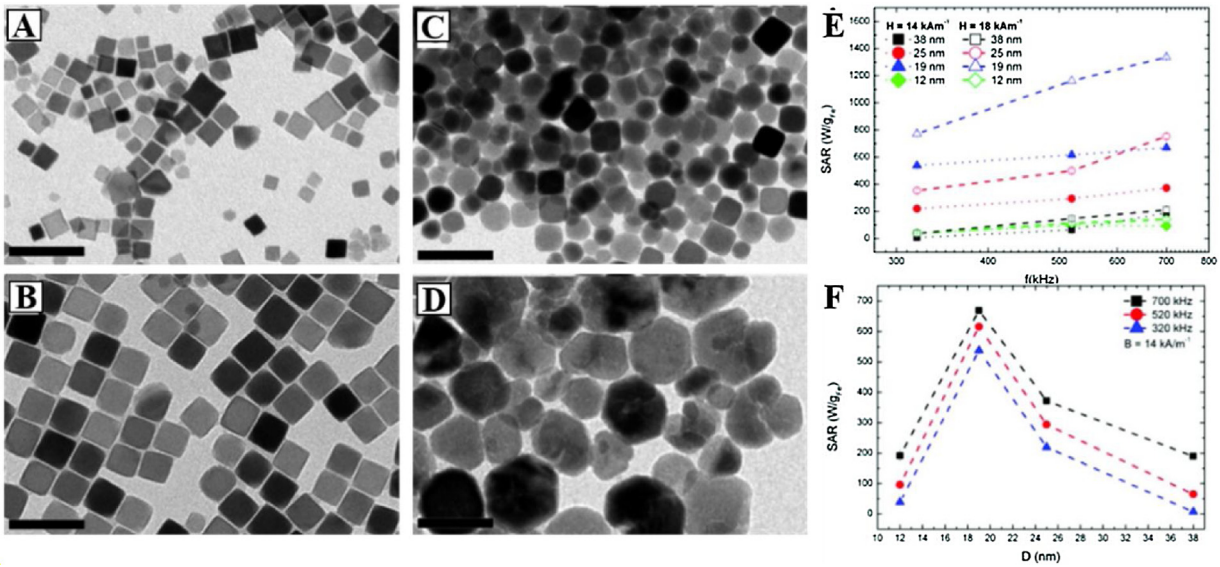

Fig. 4. Transmission electron microscopy (TEM) images of iron oxide nanocubes (IONCs) with edge lengths of (A) 12 ± 1 nm, (B) 19 ± 3 nm, (C) 25 ± 4 nm, and (D) 38 ± 9 nm. (E) Specific absorption rate (SAR) values of frequency at the two magnetic field amplitudes for four kinds of IONCs. (F) SAR values of the size of IONCs with 19 nm for three different frequencies. Reprinted with permission from ref. [120]. Copyright © 2012, American Chemical Society.

cellular component, their motion could be hampered, making Néel relaxation as the main contributor for the heat production.

There are many factors may influence the heating efficiency of the NPs, including the magnitude and frequency of the external magnetic field and the magnetic and physical properties of NPs. It has been proved that the magnetic hyperthermia efficiency could be increased with improvement of field amplitude and frequency. The impacts of nanoparticles are much more complicated because properties like diameter, magnetization, anisotropy, and homogeneity, can all affect the efficiency of heat generation [20]. Therefore, only when taking the structure, morphology, and size of magnetic NPs into consideration could high heat efficiency be achieved. Specific power adsorption rate (SAR) can represent the heating potential of different particles under different conditions. When comparing SAR values, field strength and frequency should be taken into consideration because SAR value is proportional to the field strength and frequency [118]. Begin-Colin et al. compared SAR values of different morphology of ferrite NPs (monodomain, cubes, chains and clusters) and showed a wide range from 81 Wg^{-1} to 2452 Wg^{-1}, which means the importance of regulating the nanoparticle morphology for magnetic hyperthermia application [119]. Interestingly, iron oxide nanocubes with different sizes range between 13 and 40 nm have different SAR values, and nanocubes with diameter of 19 nm have the highest values SAR values in clinical conditions and show efficient hyperthermia performance (Fig. 4) [120].

Hyperthermia accompanied by imaging techniques can improve the therapy efficiency and avoid harm to normal tissues because imaging guidance can display the targeted tumor sites and distinguish from normal tissues. Iron oxide NPs are the most common materials for hyperthermia. Many reports have demonstrated that iron oxide NPs can be the agents for MR imaging and hyperthermia [121]. Therefore, various efforts have been made to optimize the heating efficiency of iron oxide NPs. Iron oxide-based nanomaterials, such as core-shell nanostructures [122], multicore NPs [123] and nanocubes [120], were reported to generate efficient magnetic heating. Some other elements are also merged into iron oxide NP as components of heterostrctures to improve their performance. For example, $Gd_{0.02}Fe_{2.98}O_4$ NPs showed the improved hyperthermia effects with higher SAR value and ability as MRI contrast agents [124]. γ-$Mn_xFe_{2-x}O_3$ NPs seemed to be promising candidates for hyperthermia and showed higher potential as MRI contrast agents [125].

Besides, magnetic-field-induced hyperthermia can also be manipulated to combine with or as stimulus to trigger other therapies. Wilhelm et al. reported that iron oxide nanocubes with an average diameter of 20 nm can achieve heating efficiency at clinical doses (0.25 M) and acceptable irradiation (0.3 W/cm^2) under both an alternating magnetic field and NIR laser irradiation, which can then overcome the main disadvantages iron oxide nanoparticle-based magnetic hyperthermia or photothermia only (Fig. 5) [5]. Small-size iron oxide NPs can be used as gate in mesoporous materials to control drug release when applying an external stimuli, which can provide on-command feature with precise control [126]. Hu et al. constructed drug delivery system on mesoporous iron oxide NPs with payload of gas-generated perfluorohexane, which can simultaneously perform on-demand gas generation and drug release under high-frequency magnetic field [126]. Thermoresponsive copolymer coated with mesoporous silica NPs and iron oxide can trigger drug release for chemotherapy, along with hyperthermia and MRI [127].

Based on these examples, imaging-guided hyperthermia have great promise in cancer theranostics.

Imaging-guided photothermal therapy

Except magnetic-induced hyperthermia, light can also be used to product heat in cancer treatment, which is called photothermal therapy (PTT). This method is a promising cancer treatment that might eventually utilized in clinic since it can be controlled spatiotemporally to reduce their side effects. However, it also has obvious shortcomings. Firstly, it is only suitable for superficial tumors because of the limited capability of penetration in biological body. Secondly, the healthy tissue adjacent to tumor cells can be damaged because of light absorption and then lead to reduction of therapeutic effects. Luckily, nanomaterials with capability of light-activated heating can achieve high temperature in tumor sites with lower intensity of laser irradiation and no damage to surrounding healthy tissue owing to their tumor targeting properties. Moreover, the penetration depth of photothermal effect could be improved when using NIR or even longer laser wavelengths, which have lower absorption by healthy tissues, could improve the

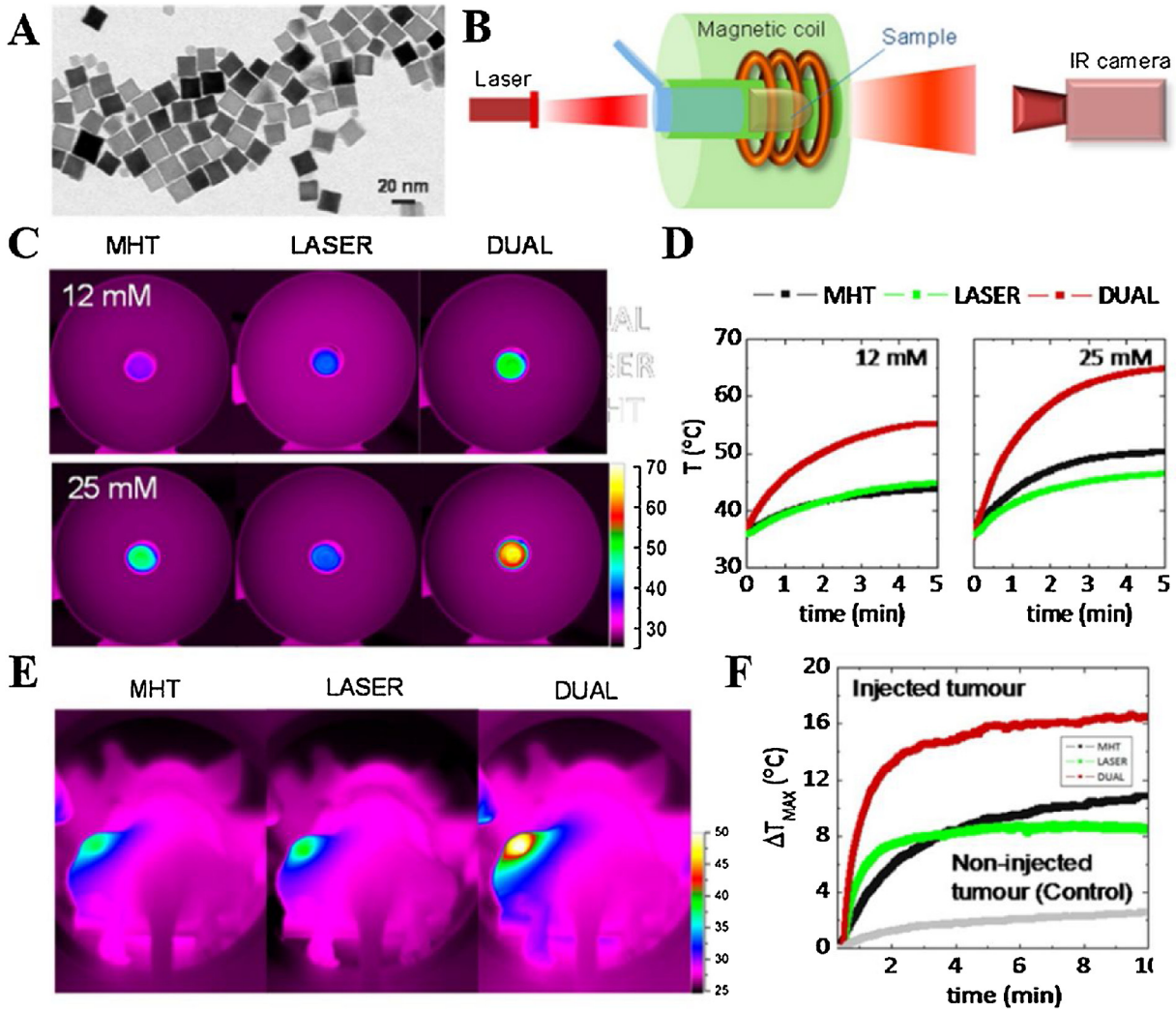

Fig. 5. (A) Transmission electron microscopy (TEM) of iron oxide nanocubes of 20 nm. (B) Scheme of the experimental device for combined photothermal and magnetic hyperthermia. (C) Thermal images achieved by the IR camera on samples with two kinds of iron concentration. (D) Temporal response curves of two different Fe concentrations with each treatment. (E) Thermal images achieved by the IR camera on mouse injected nano-samples with different treatment. (F) Corresponding temporal response curves of mouse. Reprinted with permission from ref. [5]. Copyright © 2016, American Chemical Society.

photothermal efficiency. Therefore, nanomaterials applied in PTT should have properties including large absorption cross-section of optical wavelengths, biocompatibility and low toxicity. There have been various materials employed for PTT, including noble metal-based nanomaterials [62,63], carbon-based nanomaterials [4,64], organic materials [128,129] and others [65,130].

Noble metal -based nanomaterials, using localized surface plasmon resonance (LSPR) to absorb and covert light to vibrational heat energy, have emerged as the leading PTT platform because they have facile surface functionalization for conjugating ligands to achieve targeting ability or passivating agents to improve biocompatibility. Meanwhile, their optical properties can be regulated by controlling their structural morphology and integrating other elements to form heterostrcutures so that they can absorb light maximally and penetrate deeply in tumor sites. For example, gold nanostructures with absorption peaks located in the NIR regions, such as gold nanorods, nanostars and nanocages, have shown excellent efficiency for tumor ablation with NIR light irradiation, which highlights their promise in clinic and promote the further development of PTT [131–134]. Zhang et al. synthesized thermoresponsive polymer encapsulated gold nanorods which can transfer energy from NIR laser to heat, which can almost completely inhibited tumor growth and lung metastasis [131]. Our group designed Au_3Cu tetrapod nanocrystals (TPNCs) with absorption peak totally located in the NIR-II region. They have the ability for deeper tissue PTT. They exhibited excellent photothermal performance with photothermal conversion efficiency value achieving 39.45% under 808 nm and 75.27% under 1064 nm laser irradiation. What's more, they could achieve photoacoustic imaging-guided PTT in the NIR-II region with capability of degradation and metabolizability (Fig. 6) [135].

Except noble metal-based nanomaterials, other kinds of nanomaterials can also show the ability of photothermal effect with imaging functions. Carbon NPs with sp^2 domain rich such as carbon nanotubes and graphene are well known as photothermal converting NPs. For example, Robinson et al. reported reduced graphene oxide sheets with average 20 nm lateral dimension and high NIR light absorbance potential exhibited high photothermal efficiency. [136] In addition, copper-based chalcogenides, Pd nanosheets and even organic particles are good candidate for imaging-guided PTT. Such as ultrasmall $CuCo_2S_4$ nanocrystals with size of 10 nm were synthesized and showed high photothermal performance with photothermal conversion efficiency up to 73.4% and capability for magnetic resonance (MR) imaging and infrared thermal imaging. [40] Transitional metal dichalcogenides such as MoS_2 [137,138], WS_2 [139,140] and Bi_2Se_3 [141] with high absorbance in the NIR

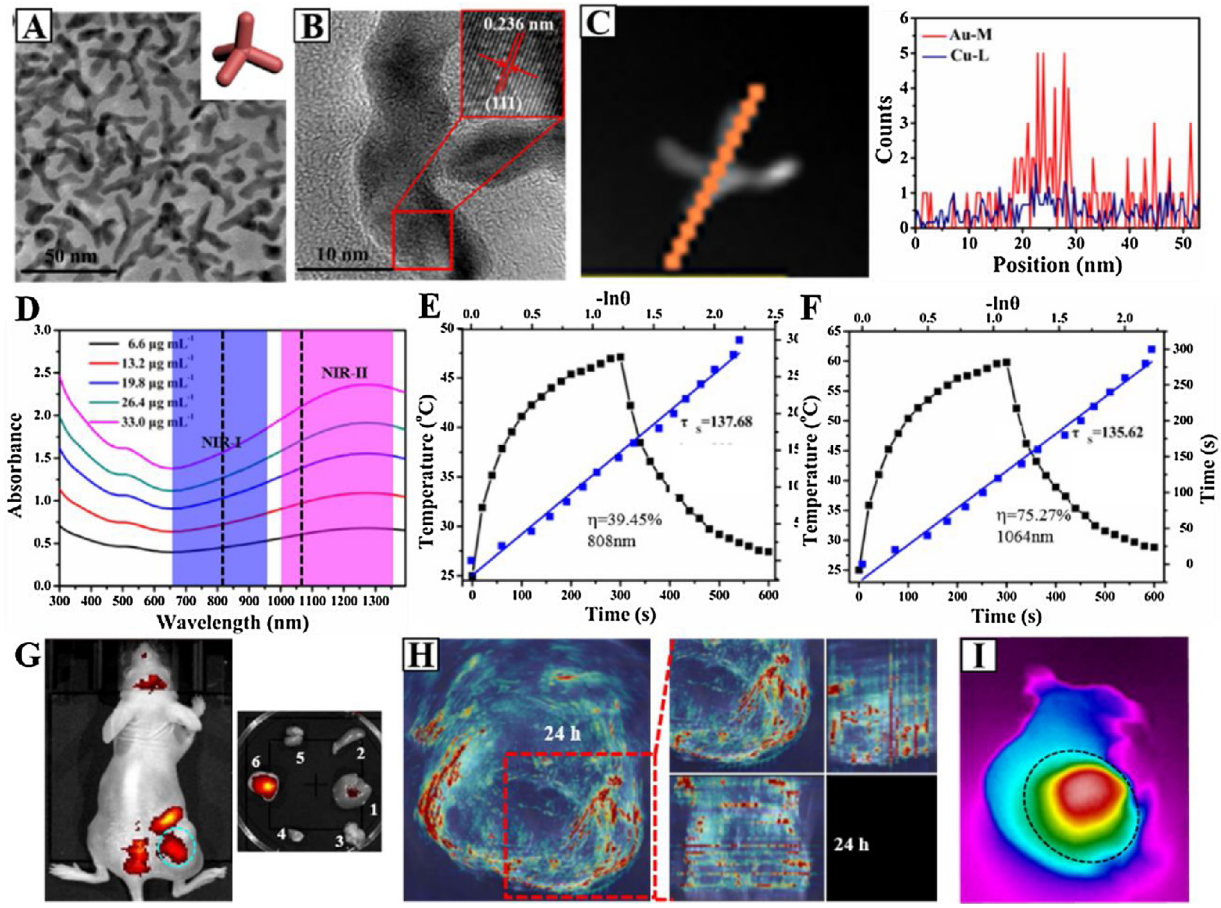

Fig. 6. (A) TEM images of Au_3Cu tetrapod nanocrystals (TPNCs), inset is the geometric model of Au_3Cu TPNCs. (B) High resolution (HR) TEM images of Au_3Cu TPNCs. (C) Energy Dispersive spectrometer (EDS) line scan of Au_3Cu TPNCs. (D) Absorption spectra of different concentrations of Au_3Cu TPNCs. (E) Calculation of the value of photothermal-conversion efficiency of Au_3Cu@PEG TPNCs at (E) 808 nm and (F) 1064 nm. (G) Fluorescence images of tumor-bearing mouse at 48 h after intravenous injection of Au_3Cu@PEG-Cy5,FA. (H) multispectral optoacoustic tomography images and (I) Thermal infrared images after 5 min laser irradiation of 1064 nm of tumor-bearing mouse at 24 h after intravenous injection of Au_3Cu@PEG-Cy5,FA. Reproduced from Ref. [135]. Copyright © 2018, The Royal Society of Chemistry.

region have been utilized in multimodel imaging and PTT for cancers.

Imaging-guided PTT will be an attractive method for cancer theranostics. However, the penetration depth of light largely hampered the clinical applications for visualized cancer therapy. Meanwhile, unpredictable physiological damages in the microenvironment also limit their further translation in clinic.

Imaging-guided photodynamic therapy

Apart from killing tumor cells by heating, light has been reported to produce oxygen in the process of light induced therapy. Photodynamic therapy (PDT), combining light, photosensitizer and oxygen together, can cause direct damage on cancer cells which are exposed to light. Because photosensitizers could transfer the optical energy to generate cytotoxic reactive oxygen species (ROS), including hydroxyl radicals (•OH), singlet oxygen ($^1O_2$) and superoxide ($•O^{2-}$), then tumor cells could be killed through cellular apoptosis or necrosis by breaking the threshold of cell [142]. The overproduction of ROS will only happen in particular cells with internalization of the photosensitizer and laser irradiation. Therefore, PDT has great promising potential in clinical cancer treatment with reduced side effects.

During the PDT procedures, imaging is necessary as guidance to make sure the localization of the photosensitizer (PS). PSs such as porphyrin, phthalocyanines and bacteriochlorin derivatives have been demonstrated the capabilities in cancer theranostics. Some of them even have been approved for clinical use [143]. However, they are limited by their photobleaching, poor biocompatibility and inability to be absorbed in NIR region, which has been hampered by penetration depth [144]. So, NIR light induced nanophotosensitizers are urgently needed and highlight the promise for cancer imaging-guided PDT treatment. Ideal photodyanmic agents should only show efficacy under light exposure with minimal dark toxicity.

In order to integrate photodynamic therapy and imaging, it is needed to synthesize NIR-light absorbed photosensitive nanomaterials. Semiconductor QDs could show better photostability and biocompatibility than organic PSs. Ge et al. reported that graphene QDs exhibit good $^1O_2$ generation capability and could be applied in simultaneous imaging and cancer treatment [66]. However, QDs have disadvantages in terms of cytotoxicity and ROS generation efficiency compared with organic PSs. Therefore, modifying semiconductor QDs with traditional PDT agents have been developed in imaging-guided PDT and to reduce the cytotoxicity of QDs [67]. Meanwhile, gold-based nanomaterials with photosensitive agents could show multiple abilities in imaging and therapy. Vesicular assemblies of gold NPs encapsulating PS Chlorine6 (Ce6) could enable NIR fluorescence/thermal/photoacoustic imaging-guided synergistic photothermal/photodynamic therapy (Fig. 7) [36].

Interestingly, Chen et al. developed gadoliniumencapsulated graphene carbon NPs (Gd@GCNs) which could work as both imaging probes and PSs. The nanoparticle-based PS showed high $^1O_2$ quantum yield, strong fluorescence and high T_1 relaxiv-

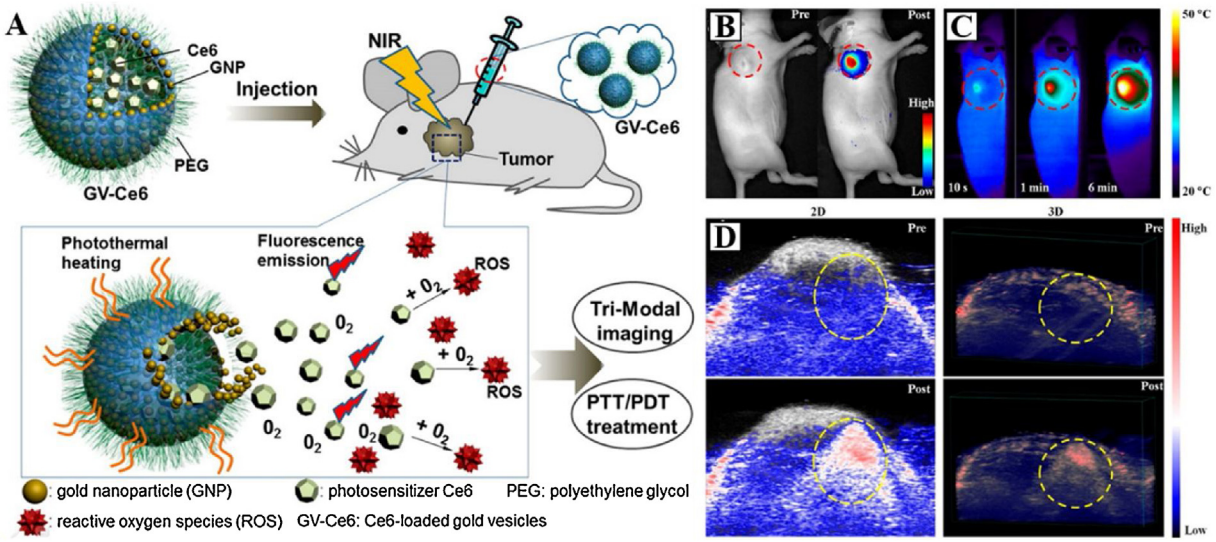

Fig. 7. (A) Scheme for photosensitizer (Ce6)-loaded gold vesicles (GVs) for fluorescence/thermal/photoacoustic imaging guided synergistic photothermal/photodynamic therapy. (B) *In vivo* NIR fluorescence images of tumor-bearing mice before and after injection of GV-Ce6. (C) Thermal images of tumor-bearing mice exposed to laser for 6 min after injection of GV-Ce6. (D) in vivo PA images before and after injection of GV-Ce6, in which yellow circles indicate the injected location of tumor. Reprinted with permission from ref. [36]. Copyright © 2013, American Chemical Society.

ity (16.0×10^{-3} $m^{-1}s^{-1}$), making them an intrinsically dual-modal imaging probe for PDT. *In vivo* experiments demonstrated the potential of the Gd@GCNs to work in the image-guided PDT for cancer treatment [68]. This work paves the way for develop of intrinsic PSs and shows that Gd@GCNs possess unique physical, pharmaceutical, and toxicological properties and are an all-in-one nanotheranostic tool with substantial clinical translation potential.

PDT has been applied in oncology for more than 30 years, however, it is only being used in the superficial treatment and cannot replace the traditional therapy. The fundamental problem lies in their chemical and physical properties lacking of biological abilities and the inability of PDT to treat solid and deep tumors. Conjugation of the photosensitizers to moieties might solve the present difficulties. And imaging–guided PDT can provide PDT direct guidance, which will ensure a promising future role in cancer treatment.

Imaging-guided chemodynamic therapy

Chemodynamic therapy (CDT), a new kind of therapeutic strategy, is defined as the disproportionation of hydrogen peroxide (H_2O_2) into ·OH, the most harmful ROS, in tumor sites through Fenton reaction or Fenton-like reaction, which can be catalyzed by ferrous ions (Fe^{2+}), iron-based nanomaterials, other metal-based nanomaterials (Mn^{2+}, Co^{2+}, and Cu^{2+}) and graphene oxide [145–148]. The TME has many distant characteristics than normal tissues, including lower pH values, overexpressed enzymes, H_2O_2 overproduction and hypoxia. These properties have already been utilized by many research to design smart nanoplatform, which can be triggered or controlled by TME, such as pH-stimuli drug delivery nanocarriers. Compared with the above cancer treatments which need to be triggered by external stimuli, CDT can be achieved by converting endogenous chemical energy into ROS and then induce cell death. Thus, CDT can break through the limitations of the penetration of light in therapy relying on laser irradiation, and avoid harm to normal tissue since the free radical can only be produced in TME.

However, the amount of H_2O_2 in tumor sites is limited and overexpressed glutathione (GSH) in tumor cells could scavenge highly reactive ·OH, thereby intrinsic catalytic efficiency is unsatisfactory and the CDT efficacy is diminished [149]. Hence, it is necessary to utilize suitable nanomaterials to improve the CDT efficiency by utilizing catalytic effect of exogenous ferrous ions. Various iron-based nanomaterials have been reported as CDT agents because they can dissolve Fe^{2+} under the mildly acidic conditions in TME and then trigger the Fenton reaction to generate ·OH inducing apoptosis and inhibiting tumor cells. Zhang et al. reported the facile synthesized amorphous iron NPs can achieve highly specific CDT with MRI guiding [69]. Wang et al. developed iron engineered mesoporous silica NPs (rFeOx-MSNs) which can also be used for in situ Fenton-like reaction to produce ·OH and cause oxidative damages to tumor cells because they can degrade into Fe^{2+}. Meanwhile, rFeOx-MSNs could be collapsed under protein-rich tissue environments because of the strong coordination between ion and proteins and then accelerate the degradation speed of iron to enhance the CDT efficacy. In addition, rFeOx-MSNs showed T_2-MRI performance for imaging because of the coexistence of Fe^{2+} and Fe^{3+}, which means they can achieve for imaging-guided CDT [70]. In addition, M(Mn, Sn, Zn)Fe_2O_4, reduced iron metal-organic framework NPs and $FeO(OH)_n$ have also been demonstrated as CDT agents [71–73,150].

Beside, other nanomaterials containing transition metal ions such as Mn^{2+}, Cu^{2+} and Co^{2+} could also act as catalytic ions [73–76]. Lin et al. reported MnO_2 coated mesoporous silica (MS@MnO_2) NPs could release Mn^{2+} in acidic environment and trigger Fenton-like activity to generate ·OH to kill tumor cells. More interestingly, Mn^{2+} yield also accompany the consuming intracellular antioxidant GSH to glutathione disulfide (GSSG), which could improve the CDT efficiency because GSH depletion made antioxidant defense system (ADS) of broken and the tumor cells more susceptible to highly toxic ·OH. Meanwhile, MS@MnO_2 NPs can be used as GSH-responsive MRI contrast agents and drug delivery systems, owing to the dissociation of MnO_2 shell to Mn^{2+} with higher T_1 relaxivity and controlling drug release under GSH stimuli. Therefore, MS@MnO_2 NPs had great potential to achieve imaging-guided chemodynamic therapeutic process (Fig. 8) [76].

Except using catalytic effect of nanomaterials, some strategies modulating of the reaction environment can also be used to optimizing the effect of CDT, like reduced pH levels, increased amounts of reactants and reduced amounts of glutathione [151–153]. Besides, exogenous energy like light, heat or magnetic fields, are also are desirable to promote the Fenton or Fenton-like reactions [146,154]. For example, since upconversion NPs showed the ability

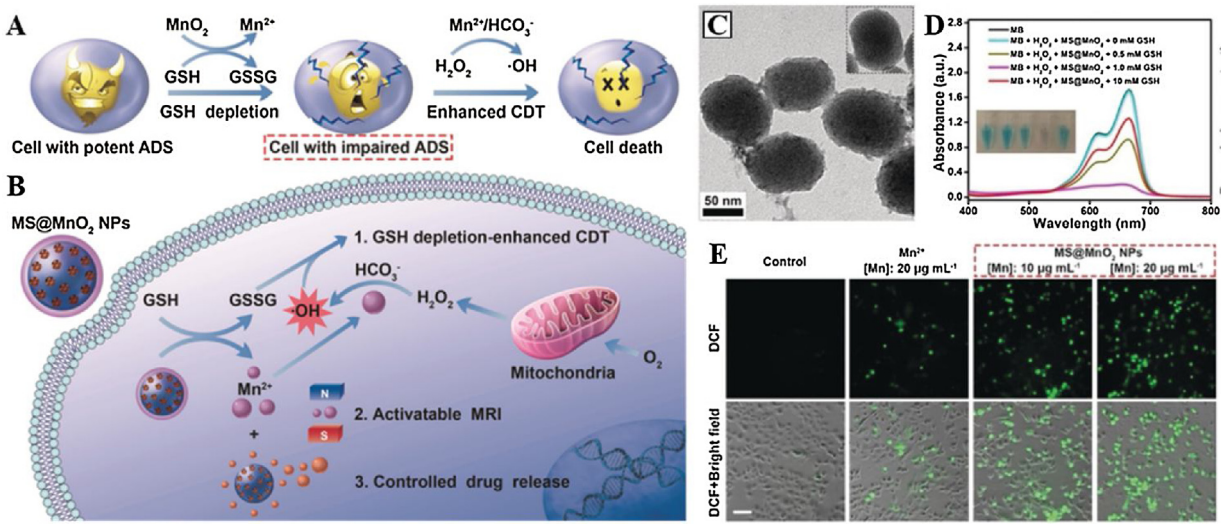

Fig. 8. (A) Schematic illustration of the mechanism of MnO_2 as chemodynamic agent for CDT in cancer. (B) The process of MnO_2 coated mesoporous silica (MS@MnO_2) NPs entered into tumor cells. (C) TEM images of MS@MnO_2 NPs and SH-MS NPs (inset) (D) Methylene blue (MB) degradation by H_2O_2 and GSH-treated MS@MnO_2 NPs. (E) DCF fluorescence images of cells incubated with Mn^{2+} and MS@MnO_2 NPs with different Mn concentrations. Scale bar: 100 μm. Reproduced with permission from ref. [76]. Copyright © 2018, Wiley-VCH Verlag GmbH & Co. KGaA, Weinheim.

of converting NIR into ultraviolet (UV) light, which promotes the Fenton reaction based on a photo Fenton reaction, Hu et al. developed a nanoplatform of $NaYF_4$:Yb^{3+},Tm^{3+}@$NaYF_4$@$dSiO_2$@$mSiO_2$-Ru^{2+}/$^{Fe2+}$ with mitochondrial DNA targeting can generate highly toxic ·OH abundantly with accumulated H_2O_2 in intratumoral mitochondrion *via* NIR-triggered photo Fenton reaction [154].

Unlike traditional cancer therapies, CDT has emerged as a new treatment using endogenous chemical energy with highly specificity and selectivity. More importantly, CDT can combine with other therapeutic treatments synthetically to destroy tumor more efficiently, having potential for clinical translation.

Imaging-guided surgery

Oncologic surgery is one of the traditional cancer treatments and is the most common part of treatment procedure for over 80% cancer patients. Surgery is the only curative choice for patients with solid tumors. It is necessary for surgeon to discriminate cancer with healthy tissue accurately during operation so that they can remove tumor cells precisely with minimal damage to normal tissues like nerves to maintain quality of life of patients. Imaging-guided surgery is one of the main methods for distinction in clinic. Before surgery, surgeon always make the specific operation plan rely on overall diagnosis results of the patient, especially imaging results which could provide the information about location, size and shape of tumor. However, as we have mentioned above, each imaging technique we use currently has their limitations, which may bring danger during the operation, and the most parts of these clinical imaging techniques cannot be utilized intraoperatively. Besides, it is very hard for surgeon to resect all tumor tissues of the patient by naked eyes because of indistinct margin between tumor and normal tissues, increasing the possibility of cancer recrudescence. Therefore, it has becoming urgent requirement to develop contrast agent for imaging-guided surgery to achieve extremely precise discrimination and resection of tumor tissues.

Optical imaging is the most direct and promising strategies to highlight cancerous cells intraoperatively and detect tumor margin with high sensitivity and specificity. Clinical applications have proven the powerful function of optical imaging to guide surgeons performing precision surgery in real-time, thus ensuring radical resection of tumors and increasing survival rates of patients. At present, the Food and Drug Administration (FDA) have approved the fluorescent dye indocyanine green (ICG) applied in hepatic micrometastases detection and sentinel lymph node mapping [77,78]. However, ICG is limited by the lack of precise targeting. In order to enable imaging agents with selectivity, fluorescent dyes can be conjugated with targeting moieties such as antibodies, peptides and sugars, which are overexpressed and accumulated in tumor sites [79].

Besides, self-illuminating NPs in the NIR region, such as QDs and carbon nanotubes, could represent another promising source for imaging-guided surgery therapy. Compared to conventional fluorescent dyes, QDs could show stronger signal and have longer fluorescence lifetime [155]. Gao et al. designed CdSe@ZnS QDs with 650 nm emission wavelength modificated by PEG and active targeting antibody. Owing to the specific optical property of QDs, illumination signal was obtained in the tumor sites after 2 h intravenous injection [156]. Carbon nanotubes have intrinsic fluorescent emission in the NIR-II window and show deeper penetration with lower influence from autofluorescene [157].

Surgeon can also rely on other optical imaging techniques to distinct margin between tumor and normal tissues and resect tumor tissues of patient. Kircher *et al.* reported a unique triple-modal MRI-PAI-Raman imaging NPs with 60-nm gold core covered with the Raman molecular tag *trans*-1,2-bis(4-pyridyl)-ethylene and further protected by a 30-nm silica coating, which can be used to guide surgeon to resect the brain tumors accurately in living mice, in which MRI can provide information for surgery planning preoperatively and Raman signal can visualize the tumor margin intraoperatively [80]. This probe could make neurosurgeons to 'see' tumor margin accurately before and during surgery, thus allowing for completely brain tumor resection according to Raman signals and subsequent histological analysis of sections (Fig. 9)

Although imaging-guided surgery have promising applications in clinic, there are still many existing problems that need to be solved, such as the long blood circulation of nanoagents are needed for clinical preoperation plans, and imaging techniques should improve spatial resolution to provide more distinct information during surgery. With those problems solved, imaging-guided surgery will have great potential in cancer imaging and therapy.

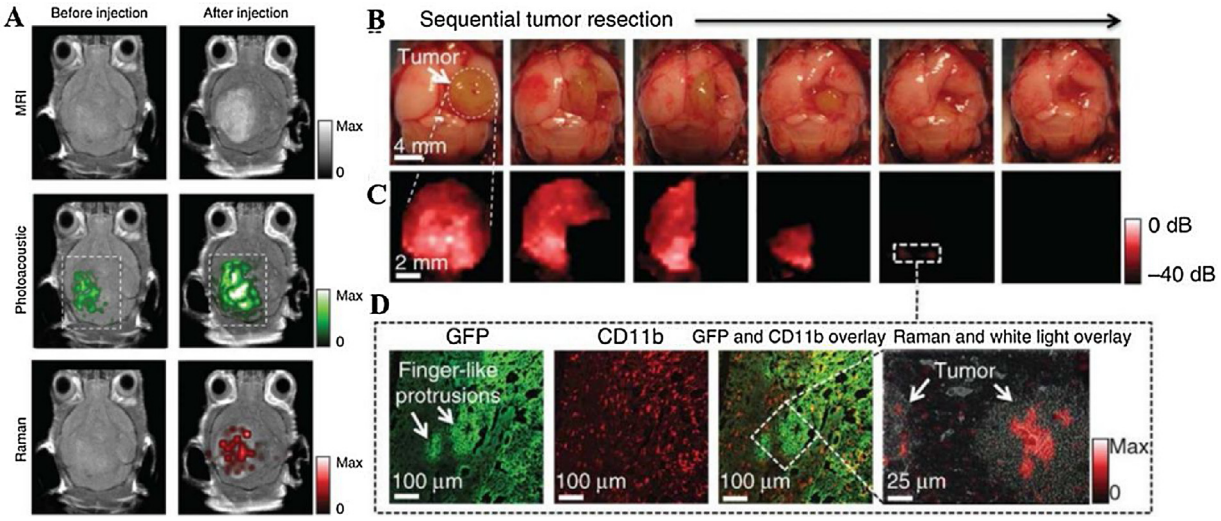

Fig. 9. (A) Two-dimensional axial MRI, photoacoustic and Raman images before and after injection. (B) Living tumor-bearing mice underwent sequential tumor resection under anesthesia. (C) Intraoperative Raman image was achieved after each resection step until the whole tumor was totally removed. (D) Histological analysis of tissue sections showed an infiltrative pattern of tumor cells in this location. Reproduced with permission from ref. [80]. Copyright © 2018, Springer Nature.

Imaging-guided multimodal synergistic therapy

Synergistic therapy could combine merits of different treatment to produce synergistic effects with higher therapeutic efficiency than any single one [158]. Therefore, the development of imaging-guided synergistic therapy is highly desirable for cancer treatment.

The combination of photothermal and chemotherapy could lead to enhanced destruction of cancer cells synergistically. Besides, the heat of photothermal effect could also trigger the system to release drug and achieve imaging-guided combination therapy [132,158,159]. Cheng et al. demonstrated a new nanosystem built on the integration of Au nanocages as carrier and photothermal agents, and lauric acid, which was a phase-change material with melting point around 43 °C. Then selenous acid, an attractive chemotherapeutic agent, could be loaded into the cavities of Au nanocages. When applying NIR laser irradiation to the nanosystem, photothermal agents melted the lauric acid and triggered the rapid release of selenous acid [160]. This study inspires us to actively control the nanoplatform as the therapeutic agents according to their intrinsic properties, which will pave the way for personalized medicine.

Radiation therapy (RT) utilizes ionizing radiation to generate oxygen radicals and attack cancer cells. However, high-energy radiation including X-ray and γ-ray may cause severe damages to normal tissues when killing cancer cells. And the hypoxic TME make tumor cells more resistant to ionizing radiation and finally the failure of RT [161,162]. MnSe@Bi_2Se_3 nanostructures were fabricated for MR and CT imaging-guided synergistic photothermal therapy and radiotherapy. In this system, the MnSe core offers T_1- and T_2-weighted MRI contrast agents, whereas Bi_2Se_3 shell endows the ability for CT imaging, enhanced RT and PTT. The NPs showed strong synergistic effect *in vivo* resulting from the remarkably increased oxygenation during PTT and enhancement of RT efficacy for effective cancer killing [163]. This work also demonstrates a promise strategy to enhance RT efficiency and the great advantages of synergistic therapy.

In addition, synergistic therapeutic effect of PDT and PTT have also been demonstrated compared to PTT or PDT alone [164,165]. Combined PTT and immunotherapy is more effective than either PTT or immunotherapy against primary treated and distant untreated tumors in a mouse tumor model [166]. This means inherent multifunctional inorganic nanoplatforms have great potential to provide more efficient cancer treatment when endowing synergistic therapeutic functions.

Conclusion and prospects

In this review, we have shown the various inorganic nanoplatforms possessing intrinsic magnetic, optical, and chemical properties capabilities for imaging-guided therapy, including magnetic hyperthermia, PTT, PDT, CDT, surgery and synergistic therapy. There are two different approaches to get these multifunctional NPs. One approach is combining multiple functional moieties together through encapsulating or conjugating or absorbing the agent to others, which increasing the complexity of nanomaterials. So this approach is hard for reproducibility, toxicity biodegradation and studies. The other one is what we focus on that engineering nanomaterials possessing intrinsically multifunctional capabilities, most of which are inorganic components with specific imaging and therapeutic abilities. This approach has great advantages in reproducibility and scale-up owing to the much simplified synthesis. These inherent functional components could be used to form core@shell heterostructure, dimer heterostructure, and multicomponent heterostructure, which could break the limitation of single component and then have wider application in imaging-guided therapy.

Owing to the imaging visualization and diagnosis, the therapeutic plan could be designed more accurately before surgery. And the treatment efficiency could also be evaluated during and re-examined after therapy. Finally, the cooperative imaging and therapeutic agents have the capability of killing cancer with minimal side effects. Therefore, with these nanomaterials, the normal cancer treatments in clinic, including diagnosis, therapy and re-examination, could be integrated into a simplified personal treatment and decrease the side effect and the cost for patients.

However, considerable efforts should be devoted continually to new methods synthesizing uniform heterostruture with intrinsically different functional components and new materials that are intrinsically multifunctional. And we cannot choose and combine functional components randomly to obtain multicomponent inherent NPs since many factors influence the synthesis process, including lattice spacing between two components, charge transfer between the seeds and newly nucleated components, seed-to-precursor ratio, reactant concentration and heating profile as we mentioned above.

Besides, several issues should be carefully considered during the development of intrinsically multifunctional nanomaterials be applied in imaging-guided therapy and in clinic in the future. Firstly, biocompatibility of nanomaterials should be guaranteed for their further application *in vivo*. So nanomaterials should be suitably modificated to ensure they can disperse and keep stable in water. It is worth mentioning that natural materials from the human body are safer than synthetic materials for clinical purposes [167–169]. Secondly, *in vivo* targeting efficacy of imaging agents is very important. Sufficient amounts of imaging agents should be accumulated in the target tumor sites in order to obtain successful results in imaging and therapy. According to previous studies, the metabolism processes *in vivo* of nanomaterial is quite related with their sizes. NPs with sizes larger than 100 nm would be accumulated in liver and spleen owing to the capture of the reticuloendothelial system (RES), while NPs with sizes smaller than 10 nm will be easily cleared by the kidney during the systemic circulation. Therefore, those with sizes around 10–100 nm would have advantages in nanomedicine because they may have favourable behavior of biodistribution, accumulation and clearance. Thirdly, toxicity studies of the nanomaterials need to be addressed before they can be used in clinic. The physicochemical properties of NPs are essential to be optimized during the design, and therefore they can show favorable biodistribution with minimal RES elimination. Finally, metabolism of nanomaterials should be studied furtherly. It would not be better that nanomaterials could be degraded into clearable components and elimination from body. However, nanomaterials which cannot be degraded or removed by the body, have potential to harm the human bodies as they would be captured and accumulated by the RES. Moreover, the metabolic pathway of nanomaterials is still not completely understood at the molecular level, so many studies should be performed before we could totally control the behavior of nanomaterials. It would be a good opportunity to accelerate product entry into clinical practice when using FDA approved components to engineering inherent multifunctional nanomaterials.

The continued development of such intrinsically multifunctional inorganic nanomaterials is increasingly important and will open the era of cancer diagnosis and therapy in clinic in the future. We believe that these nanomaterials will help us to achieve personalized medicine since they could be synthesized according to our request and plan. Cancer patients may have opportunity for recovery from fatal disease and finally come into optimistic outlook in future.

Acknowledgements

This work was financially supported by the Natural Science Foundation Beijing of Municipality (L172008), the National Natural Science Foundation of China (51672010, 81421004, 51631001, 51590882, 51602285), the National Key R&D Program of China (2017YFA0206301, 2016YFA0200102). Young Elite Scientist Sponsorship Program by CAST (2017QNRC001). Fund of Key Laboratory of Advanced Materials of Ministry of Education (53220330118).

References

[1] R.L. Siegel, K.D. Miller, A. Jemal, CA-Cancer J. Clin. 67 (2017) 7.
[2] J.W. Valle, A. Armstrong, C. Newman, V. Alakhov, G. Pietrzynski, J. Brewer, S. Campbell, P. Corrie, E.K. Rowinsky, M. Ranson, Invest. New Drug 29 (2011) 1029.
[3] S. Danson, D. Ferry, V. Alakhov, J. Margison, D. Kerr, D. Jowle, M. Brampton, G. Halbert, M. Ranson, Brit. J. Cancer 90 (2004) 2085.
[4] C. Liang, S. Diao, C. Wang, H. Gong, T. Liu, G.S. Hong, X.Z. Shi, H.J. Dai, Z. Liu, Adv. Mater. 26 (2014) 5646.
[5] A. Espinosa, R. Di Corato, J. Kolosnjaj-Tabi, P. Flaud, T. Pellegrino, C. Wilhelm, ACS Nano 10 (2016) 2436.
[6] C. Blanco-Andujar, D. Ortega, P. Southern, Q.A. Pankhurst, N.T.K. Thanh, Nanoscale 7 (2015) 1768.
[7] P. Juzenas, W. Chen, Y.P. Sun, M.A.N. Coelho, R. Generalov, N. Generalova, I.L. Christensen, Adv. Drug Deliver. Rev. 60 (2008) 1600.
[8] X. Wang, H.R. Chen, K. Zhang, M. Ma, F.Q. Li, D.P. Zeng, S.G. Zheng, Y. Chen, L.X. Jiang, H.X. Xu, J.L. Shi, Small 10 (2014) 1403.
[9] C.Y. Liu, J. Guo, W.L. Yang, J.H. Hu, C.C. Wang, S.K. Fu, J. Mater. Chem. 19 (2009) 4764.
[10] D.K. Chatterjee, L.S. Fong, Y. Zhang, Adv. Drug Deliver. Rev. 60 (2008) 1627.
[11] R. Sharma, N. Mody, U. Agrawal, S.P. Vyas, Mini-Rev. Med. Chem. 17 (2017) 1746.
[12] D.B. Chithrani, S. Jelveh, F. Jalali, M. van Prooijen, C. Allen, R.G. Bristow, R.P. Hill, D.A. Jaffray, Radiat. Res. 173 (2010) 719.
[13] X.H. Sun, G.D. Zhang, R.S. Keynton, M.G. O'Toole, D. Patel, A.M. Gobin, Nanomed. Nanotechnol. Biol. Med. 9 (2013) 1214.
[14] L. Maggiorella, G. Barouch, C. Devaux, A. Pottier, E. Deutsch, J. Bourhis, E. Borghi, L. Levy, Future Oncol. 8 (2012) 1167.
[15] H. Maeda, J. Wu, T. Sawa, Y. Matsumura, K. Hori, J. Control. Release 65 (2000) 271.
[16] Y. Wang, G.Q. Wei, X.B. Zhang, F.N. Xu, X. Xiong, S.B. Zhou, Adv. Mater. 29 (2017) 10.
[17] J.L. Geng, K. Li, D. Ding, X.H. Zhang, W. Qin, J.Z. Liu, B.Z. Tang, B. Liu, Small 8 (2012) 3655.
[18] J.H. Kim, Y.S. Kim, K. Park, E. Kang, S. Lee, H.Y. Nam, K. Kim, J.H. Park, D.Y. Chi, R.W. Park, I.S. Kim, K. Choi, I.C. Kwon, Biomaterials 29 (2008) 1920.
[19] D.T. Wiley, P. Webster, A. Gale, M.E. Davis, Proc. Natl. Acad. Sci. U. S. A. 110 (2013) 8662.
[20] J. Yu, X. Chu, Y.L. Hou, Chem. Commun. 50 (2014) 11614.
[21] H.B. Na, I.C. Song, T. Hyeon, Adv. Mater. 21 (2009) 2133.
[22] J.H. Gao, H.W. Gu, B. Xu, Accounts. Chem. Res. 42 (2009) 1097.
[23] N. Sanvicens, M.P. Marco, Trends Biotechnol. 26 (2008) 425.
[24] S. Sevenson, D.A. Tomalia, Adv. Drug Deliver. Rev. 64 (2012) 102.
[25] D. Peer, J.M. Karp, S. Hong, O.C. FaroKhzad, R. Margalit, R. Langer, Nat. Nanotechnol. 2 (2007) 751.
[26] J.C. Li, K.Y. Pu, Chem. Soc. Rev. 48 (2019) 38.
[27] Y.Y. Jiang, K.Y. Pu, Accounts. Chem. Res. 51 (2018) 1840.
[28] Q.Q. Miao, K.Y. Pu, Adv. Mater. 30 (2018) 23.
[29] Y. Lyu, D. Cui, H. Sun, Y.S. Miao, H.W. Duan, K.Y. Pu, Angew. Chem. Int. Ed. 56 (2017) 9155.
[30] J.C. Li, X. Zhen, Y. Lyu, Y.Y. Jiang, J.G. Huang, K.Y. Pu, ACS Nano 12 (2018) 8520.
[31] H.J. Zhu, J.C. Li, X.Y. Qi, P. Chen, K.Y. Pu, Nano Lett. 18 (2018) 586.
[32] M.K. Yu, Y.Y. Jeong, J. Park, S. Park, J.W. Kim, J.J. Min, K. Kim, S. Jon, Angew. Chem. Int. Ed. 120 (2008) 5442.
[33] X. Ren, R. Zheng, X. Fang, X. Wang, X. Zhang, W. Yang, X. Sha, Biomaterials 92 (2016) 13.
[34] N. Khlebtsov, L. Dykman, Chem. Soc. Rev. 40 (2011) 1647.
[35] D. Kim, Y.Y. Jeong, S. Jon, ACS Nano 4 (2010) 3689.
[36] J. Lin, S. Wang, P. Huang, Z. Wang, S. Chen, G. Niu, W. Li, J. He, D. Cui, G. Lu, ACS Nano 7 (2013) 5320.
[37] X.J. Wang, C. Wang, L. Cheng, S.T. Lee, Z. Liu, J. Am. Chem. Soc. 134 (2012) 7414.
[38] H.Q. Tao, K. Yang, Z. Ma, J.M. Wan, Y.J. Zhang, Z.H. Kang, Z. Liu, Small 8 (2012) 281.
[39] Z.L. Li, J. Liu, Y. Hu, Z. Li, X.L. Fan, Y. Sun, F. Besenbacher, C. Chen, M. Yu, Biomaterials 141 (2017) 284.
[40] B. Li, F.K. Yuan, G.J. He, X.Y. Han, X. Wang, J.B. Qin, Z.X. Guo, X.W. Lu, Q. Wang, I.P. Parkin, C.T. Wu, Adv. Funct. Mater. 27 (2017) 10.
[41] G. Lv, W. Guo, W. Zhang, T. Zhang, S. Li, S. Chen, A.S. Eltahan, D. Wang, Y. Wang, J. Zhang, ACS Nano 10 (2016) 9637.
[42] Y.W. Jun, Y.M. Huh, J.S. Choi, J.H. Lee, H.T. Song, S. Kim, S. Yoon, K.S. Kim, J.S. Shin, J.S. Suh, J. Cheon, J. Am. Chem. Soc. 127 (2005) 5732.
[43] M.A. Fortin, R.M. Petoral, F. Soderlind, A. Klasson, M. Engstrom, T. Veres, P.O. Kall, K. Uvdal, Nanotechnology 18 (2007) 9.
[44] F. Evanics, P.R. Diamente, F. van Veggel, G.J. Stanisz, R.S. Prosser, Chem. Mater. 18 (2006) 2499.
[45] H. Hifumi, S. Yamaoka, A. Tanimoto, D. Citterio, K. Suzuki, J. Am. Chem. Soc. 128 (2006) 15090.
[46] H.B. Na, J.H. Lee, K.J. An, Y.I. Park, M. Park, I.S. Lee, D.H. Nam, S.T. Kim, S.H. Kim, S.W. Kim, K.H. Lim, K.S. Kim, S.O. Kim, T. Hyeon, Angew. Chem. Int. Ed. 46 (2007) 5397.
[47] M. Shilo, T. Reuveni, M. Motiei, R. Popovtzer, Nanomedicine 7 (2012) 257.
[48] C. Kojima, Y. Umeda, M. Ogawa, A. Harada, Y. Magata, K. Kono, Nanotechnology 21 (2010) 6.
[49] O. Rabin, J.M. Perez, J. Grimm, G. Wojtkiewicz, R. Weissleder, Nat. Mater. 5 (2006) 118.
[50] P.J. Bonitatibus, A.S. Torres, G.D. Goddard, P.F. FitzGerald, A.M. Kulkarni, Chem. Commun. 46 (2010) 8956.
[51] J.L. Li, B. Tang, B. Yuan, L. Sun, X.G. Wang, Biomaterials 34 (2013) 9519.
[52] M. He, P. Huang, C. Zhang, H. Hu, C. Bao, G. Gao, R. He, D. Cui, Adv. Funct. Mater. 21 (2011) 4470.
[53] C. Farrera, F.T. Andon, N. Feliu, ACS Nano 11 (2017) 10637.
[54] C.J. Murphy, A.M. Gole, J.W. Stone, P.N. Sisco, A.M. Alkilany, E.C. Goldsmith, S.C. Baxter, Accounts Chem. Res. 41 (2008) 1721.
[55] X.L. Sun, W.B. Cai, X.Y. Chen, Accounts Chem. Res. 48 (2015) 286.
[56] S.M. Janib, A.S. Moses, J.A. MacKay, Adv. Drug Deliver. Rev. 62 (2010) 1052.

[57] W. Lu, Q. Huang, K.B. Geng, X.X. Wen, M. Zhou, D. Guzatov, P. Brecht, R. Su, A. Oraevsky, L.V. Wang, C. Li, Biomaterials 31 (2010) 2617.
[58] B.R. Smith, S.S. Gambhir, Chem. Rev. 117 (2017) 901.
[59] R.K. Gilchrist, R. Medal, W.D. Shorey, R.C. Hanselman, J.C. Parrott, C.B. Taylor, Ann. Surg. 146 (1957) 596.
[60] L. Asin, M.R. Ibarra, A. Tres, G.F. Goya, Pharmaceut. Res. 29 (2012) 1319.
[61] M. Johannsen, B. Thiesen, P. Wust, A. Jordan, Int. J. Hyperthermia 26 (2010) 790.
[62] Z.H. Bao, X.R. Liu, Y.D. Liu, H.Z. Liu, K. Zhao, Asian J. Pharm. Sci. 11 (2016) 349.
[63] M. Zhou, M. Tian, C. Li, Bioconjugate. Chem. 27 (2016) 1188.
[64] G.S. Hong, S.O. Diao, A.L. Antaris, H.J. Dai, Chem. Rev. 115 (2015) 10816.
[65] J. Liu, X.P. Zheng, Z.J. Gu, C.Y. Chen, Y.L. Zhao, Nanomed. Nanotechnol. Biol. Med. 12 (2016) 486.
[66] J.C. Ge, M.H. Lan, B.J. Zhou, W.M. Liu, L. Guo, H. Wang, Q.Y. Jia, G.L. Niu, X. Huang, H.Y. Zhou, X.M. Meng, P.F. Wang, C.S. Lee, W.J. Zhang, X.D. Han, Nat. Commun. 5 (2014) 8.
[67] I.V. Martynenko, V.A. Kuznetsova, A.O. Orlova, P.A. Kanaev, V.G. Maslov, A. Loudon, V. Zaharov, P. Parfenov, Y.K. Gun'ko, A.V. Baranov, A.V. Fedorov, Nanotechnology 26 (2015) 9.
[68] H.M. Chen, Y.W. Qiu, D.D. Ding, H.R. Lin, W.J. Sun, G.D. Wang, W.C. Huang, W.Z. Zhang, D. Lee, G. Liu, J. Xie, X. Chen, Adv. Mater. 30 (2018) 9.
[69] C. Zhang, W.B. Bu, D.L. Ni, S.J. Zhang, Q. Li, Z.W. Yao, J.W. Zhang, H.L. Yao, Z. Wang, J.L. Shi, Angew. Chem. Int. Ed. 55 (2016) 2101.
[70] L.Y. Wang, M.F. Huo, Y. Chen, J.L. Shi, Biomaterials 163 (2018) 1.
[71] K.T. Lee, Y.J. Lu, F.L. Mi, T. Burnouf, Y.T. Wei, S.C. Chiu, E.Y. Chuang, S.Y. Lu, ACS Appl. Mater. Inter. 9 (2017) 1273.
[72] D. Cioloboc, C. Kennedy, E.N. Boice, E.R. Clark, D.M. Kurtz, Biomacromolecules 19 (2018) 178.
[73] H. Ranji-Burachaloo, F. Karimi, R. Xie, Q. Fu, P.A. Gurr, D.E. Dunstan, G.G. Qiao, ACS Appl. Mater. Inter. 9 (2017) 33599.
[74] M.F. Poyton, A.M. Sendecki, X. Cong, P.S. Cremer, J. Am. Chem. Soc. 138 (2016) 1584.
[75] A.H. Xu, X.X. Li, S.A. Ye, G.C. Yin, Q.F. Zeng, Appl. Catal. B Environ. 102 (2011) 37.
[76] L.S. Lin, J.B. Song, L. Song, K.M. Ke, Y.J. Liu, Z.J. Zhou, Z.Y. Shen, J. Li, Z. Yang, W. Tang, G. Niu, H.H. Yang, X.Y. Chen, Angew. Chem. Int. Ed. 57 (2018) 4902.
[77] M.N. Loja, Z. Luo, D.G. Farwell, Q.C. Luu, P.J. Donald, D. Amott, A.Q. Truong, R.F. Gandour-Edwards, N. Nitin, Int. J. Cancer 132 (2013) 1613.
[78] N. Yokoyama, T. Otani, H. Hashidate, C. Maeda, T. Katada, N. Sudo, S. Manabe, Y. Ikeno, A. Toyoda, N. Katayanagi, Cancer 118 (2012) 2813.
[79] E.M. Sevick-Muraca, Translation of near-infrared fluorescence imaging technologies: emerging clinical applications, in: C.T. Caskey, C.P. Austin, J.A. Hoxie (Eds.), Annual Review of Medicine, Vol 63, Annual Reviews, Palo Alto, 2012, p. 217.
[80] M.F. Kircher, A. de la Zerda, J.V. Jokerst, C.L. Zavaleta, P.J. Kempen, E. Mittra, K. Pitter, R.M. Huang, C. Campos, F. Habte, R. Sinclair, C.W. Brennan, I.K. Mellinghoff, E.C. Holland, S.S. Gambhir, Nat. Med. 18 (2012) 829.
[81] M.B. Cortie, A.M. McDonagh, Chem. Rev. 111 (2011) 3713.
[82] D.S. Wang, Y.D. Li, Adv. Mater. 23 (2011) 1044.
[83] H. Zeng, S.H. Sun, Adv. Funct. Mater. 18 (2008) 391.
[84] S. Kango, S. Kalia, A. Celli, J. Njuguna, Y. Habibi, R. Kumar, Prog. Polym. Sci. 38 (2013) 1232.
[85] Z.C. Xu, Y.L. Hou, S.H. Sun, J. Am. Chem. Soc. 129 (2007) 8698.
[86] Y.M. Ju, H.L. Zhang, J. Yu, S.Y. Tong, N. Tian, Z.Y. Wang, X.B. Wang, X.T. Su, X. Chu, J. Lin, Y. Ding, G.J. Li, F.G. Sheng, Y.L. Hou, ACS Nano 11 (2017) 9239.
[87] J. Yu, C. Yang, J. Li, Y. Ding, L. Zhang, M.Z. Yousaf, J. Lin, R. Pang, L. Wei, L. Xu, Adv. Mater. 26 (2014) 4114.
[88] M. Mahmoudi, V. Serpooshan, S. Laurent, Nanoscale 3 (2011) 3007.
[89] J.K. Willmann, N. van Bruggen, L.M. Dinkelborg, S.S. Gambhir, Nat. Rev. Drug Discov. 7 (2008) 591.
[90] M.G. Harisinghani, J. Barentsz, P.F. Hahn, W.M. Deserno, S. Tabatabaei, C.H. van de Kaa, J. de la Rosette, R. Weissleder, New Engl. J. Med. 348 (2003) 2491.
[91] M. Arruebo, R. Fernandez-Pacheco, M.R. Ibarra, J. Santamaria, Nano Today 2 (2007) 22.
[92] T. Skotland, T.G. Iversen, K. Sandvig, Nanomed. Nanotechnol. Biol. Med. 6 (2010) 730.
[93] K. Welsher, S.P. Sherlock, H.J. Dai, Proc. Natl. Acad. Sci. U. S. A. 108 (2011) 8943.
[94] H. Gong, R. Peng, Z. Liu, Adv. Drug Deliver. Rev. 65 (2013) 1951.
[95] S.Y. Xu, J.B. Cui, L.Y. Wang, Trac Trends Anal. Chem. 80 (2016) 149.
[96] A. Polyak, T.L. Ross, Curr. Med. Chem. 25 (2018) 4328.
[97] A. Rahmim, H. Zaidi, Nucl. Med. Commun. 29 (2008) 193.
[98] J. Weber, P.C. Beard, S.E. Bohndiek, Nat. Methods 13 (2016) 639.
[99] X.D. Wang, Y.J. Pang, G. Ku, X.Y. Xie, G. Stoica, L.H.V. Wang, Nat. Biotechnol. 21 (2003) 803.
[100] S. Mallidi, T. Larson, J. Tam, P.P. Joshi, A. Karpiouk, K. Sokolov, S. Emelianov, Nano Lett. 9 (2009) 2825.
[101] U.I. Tromsdorf, O.T. Bruns, S.C. Salmen, U. Beisiegel, H. Weller, Nano Lett. 9 (2009) 4434.
[102] F.Q. Hu, Q.J. Jia, Y.L. Li, M.Y. Gao, Nanotechnology 22 (2011) 7.
[103] Y.X.J. Wang, World J. Gastroenterol. 21 (2015) 13400.
[104] X. Zhen, C.W. Zhang, C. Xie, Q.Q. Miao, K.L. Lim, K.Y. Pu, ACS Nano 10 (2016) 6400.
[105] Q.Q. Miao, C. Xie, X. Zhen, Y. Lyu, H.W. Duan, X.G. Liu, J.V. Jokerst, K.Y. Pu, Nat. Biotechnol. 35 (2017) 1102.
[106] R.Z. Seeni, X.J. Yu, H. Chang, P. Chen, L.B. Liu, C.J. Xu, ACS Appl. Mater. Inter. 9 (2017) 20340.
[107] D. Shao, X. Zhang, W.L. Liu, F. Zhang, X. Zheng, P. Qiao, J. Li, W.F. Dong, L. Chen, ACS Appl. Mater. Inter. 8 (2016) 4303.
[108] L.A. Lane, X.M. Qian, S.M. Nie, Chem. Rev. 115 (2015) 10489.
[109] Y. Yang, Q. Shao, R. Deng, C. Wang, X. Teng, K. Cheng, Z. Cheng, L. Huang, Z. Liu, X. Liu, Angew. Chem. Int. Ed. 51 (2012) 3125.
[110] A.L. Antaris, H. Chen, K. Cheng, Y. Sun, G.S. Hong, C.R. Qu, S. Diao, Z.X. Deng, X.M. Hu, B. Zhang, X.D. Zhang, O.K. Yaghi, Z.R. Alamparambil, X.C. Hong, Z. Cheng, H.J. Dai, Nat. Mater. 15 (2016) 235.
[111] T.C. Lai, Y. Bae, T. Yoshida, K. Kataoka, G.S. Kwon, Pharmaceutical Res. 27 (2010) 2260.
[112] K. Wu, M. Politis, S.S. O'Sullivan, A.D. Lawrence, S. Warsi, S. Bose, A.J. Lees, P. Piccini, J. Neurol. 262 (2015) 1504.
[113] N. Tolboom, W.M. van der Flier, J. Boverhoff, M. Yaqub, M.P. Wattjes, P.G. Raijmakers, F. Barkhof, P. Scheltens, K. Herholz, A.A. Lammertsma, B.N.M. van Berckel, J. Neurol. Neurosurg. Psychiatry 81 (2010) 882.
[114] Y.C. Wang, R.C. Liang, F. Fang, J. Nanosci. Nanotechnol. 15 (2015) 5487.
[115] K.K. Wong, L.M. Fig, M.D. Gross, B.A. Dwamena, Nucl. Med. Commun. 36 (2015) 363.
[116] N. Doge, S. Honzke, F. Schumacher, B. Balzus, M. Colombo, S. Hadam, F. Rancan, U. Blume-Peytavi, M. Schafer-Korting, A. Schindler, E. Ruhl, P.S. Skov, M.K. Church, S. Hedtrich, B. Kleuser, R. Bodmeier, A. Vogt, J. Control. Release 242 (2016) 25.
[117] L.S. Goldstein, M.W. Dewhirst, M. Repacholi, L. Kheifets, Int. J. Hyperthermia 19 (2003) 373.
[118] M. Ma, Y. Wu, H. Zhou, Y.K. Sun, Y. Zhang, N. Gu, J. Magn. Magn. Mater. 268 (2004) 33.
[119] C. Blanco-Andujar, A. Walter, G. Cotin, C. Bordeianu, D. Mertz, D. Felder-Flesch, S. Begin-Colin, Nanomedicine 11 (2016) 1889.
[120] P. Guardia, R. Di Corato, L. Lartigue, C. Wilhelm, A. Espinosa, M. Garcia-Hernandez, F. Gazeau, L. Manna, T. Pellegrino, ACS Nano 6 (2012) 3080.
[121] A.K. Gupta, M. Gupta, Biomaterials 26 (2005) 3995.
[122] J.H. Lee, J.T. Jang, J.S. Choi, S.H. Moon, S.H. Noh, J.W. Kim, J.G. Kim, I.S. Kim, K.I. Park, J. Cheon, Nat. Nanotechnol. 6 (2011) 418.
[123] L. Lartigue, P. Hugounenq, D. Alloyeau, S.P. Clarke, M. Levy, J.C. Bacri, R. Bazzi, D.F. Brougham, C. Wilhelm, F. Gazeau, ACS Nano 6 (2012) 10935.
[124] P. Drake, H.J. Cho, P.S. Shih, C.H. Kao, K.F. Lee, C.H. Kuo, X.Z. Lin, Y.J. Lin, J. Mater. Chem. 17 (2007) 4914.
[125] N.K. Prasad, K. Rathinasamy, D. Panda, D. Bahadur, J. Mater. Chem. 17 (2007) 5042.
[126] P. Saint-Cricq, S. Deshayes, J.I. Zink, A.M. Kasko, Nanoscale 7 (2015) 13168.
[127] A. Baeza, E. Guisasola, E. Ruiz-Hernandez, M. Vallet-Regi, Chem. Mater. 24 (2012) 517.
[128] Y. Yang, J.J. Liu, C. Liang, L.Z. Feng, T.T. Fu, Z.L. Dong, Y. Chao, Y.G. Li, G. Lu, M.W. Chen, Z. Liu, ACS Nano 10 (2016) 2774.
[129] H.S. Jung, P. Verwilst, A. Sharma, J. Shin, J.L. Sessler, J.S. Kim, Chem. Soc. Rev. 47 (2018) 2280.
[130] Y. Ju, H. Zhang, J. Yu, S. Tong, N. Tian, Z. Wang, X. Wang, X. Su, X. Chu, J. Lin, Y. Ding, G. Li, F. Sheng, Y. Hou, ACS Nano 11 (2017) 9239.
[131] Z. Zhang, J. Wang, X. Nie, T. Wen, Y. Ji, X. Wu, Y. Zhao, C. Chen, J. Am. Chem. Soc. 136 (2014) 7317.
[132] A.M. Alkilany, L.B. Thompson, S.P. Boulos, P.N. Sisco, C.J. Murphy, Adv. Drug Deliver. Rev. 64 (2012) 190.
[133] H. Yuan, A.M. Fales, T. Vo-Dinh, J. Am. Chem. Soc. 134 (2012) 11358.
[134] S.E. Skrabalak, J. Chen, Y. Sun, X. Lu, L. Au, C.M. Cobley, Y. Xia, Accounts. Chem. Res. 41 (2008) 1587.
[135] Z.Y. Wang, Y.M. Ju, S.Y. Tong, H.C. Zhang, J. Lin, B.D. Wang, Y.L. Hou, Nanoscale Horiz. 3 (2018) 9.
[136] J.T. Robinson, S.M. Tabakman, Y.Y. Liang, H.L. Wang, H.S. Casalongue, D. Vinh, H.J. Dai, J. Am. Chem. Soc. 133 (2011) 6825.
[137] T. Liu, S.X. Shi, C. Liang, S.D. Shen, L. Cheng, C. Wang, X.J. Song, S. Goel, T.E. Barnhart, W.B. Cai, Z. Liu, ACS Nano 9 (2015) 950.
[138] L.D. Kong, L.X. Xing, B.Q. Zhou, L.F. Du, X.Y. Shi, ACS Appl. Mater. Inter. 9 (2017) 15995.
[139] L. Cheng, J.J. Liu, X. Gu, H. Gong, X.Z. Shi, T. Liu, C. Wang, X.Y. Wang, G. Liu, H.Y. Xing, W.B. Bu, B.Q. Sun, Z. Liu, Adv. Mater. 26 (2014) 1886.
[140] X.D. Song, W.T. Shang, L. Peng, H.M. Jiang, K. Wang, C.H. Fang, J. Tian, Nanomedicine 13 (2018) 1681.
[141] H.H. Xie, Z.B. Li, Z.B. Sun, J.D. Shao, X.F. Yu, Z.N. Guo, J.H. Wang, Q.L. Xiao, H.Y. Wang, Q.Q. Wang, H. Zhang, P.K. Chu, Small 12 (2016) 4136.
[142] Y.H. Cheng, H. Cheng, C.X. Jiang, X.F. Qiu, K.K. Wang, W. Huan, A. Yuan, J.H. Wu, Y.Q. Hu, Nat. Commun. 6 (2015) 8.
[143] J.F. Lovell, T.W.B. Liu, J. Chen, G. Zheng, Chem. Rev. 110 (2010) 2839.
[144] Z. Huang, Technol. Cancer Res. Treat. 4 (2005) 283.
[145] X.J. Zhou, Y. Zhang, C. Wang, X.C. Wu, Y.Q. Yang, B. Zheng, H.X. Wu, S.W. Guo, J.Y. Zhang, ACS Nano 6 (2012) 6592.
[146] Z.M. Tang, H.L. Zhang, Y.Y. Liu, D.L. Ni, H. Zhang, J.W. Zhang, Z.W. Yao, M.Y. He, J.L. Shi, W.B. Bu, Adv. Mater. 29 (2017) 8.
[147] Y.X. Liu, Q. Jia, Q.W. Guo, W. Wei, J. Zhou, Biomaterials 180 (2018) 104.
[148] Z. Tang, Y. Liu, M. He, W. Bu, Angew. Chem. Int. Ed. (2018).
[149] R. Kumar, W.S. Shin, K. Sunwoo, W.Y. Kim, S. Koo, S. Bhuniya, J.S. Kim, Chem. Soc. Rev. 44 (2015) 6670.
[150] J. Kim, H.R. Cho, H. Jeon, D. Kim, C. Song, N. Lee, S.H. Choi, T. Hyeon, J. Am. Chem. Soc. 139 (2017) 10992.

[151] Y.L. Liu, X.Y. Ji, W.W.L. Tong, D. Askhatova, T.Y. Yang, H.W. Cheng, Y.Z. Wang, J.J. Shi, Angew. Chem. Int. Ed. 57 (2018) 1510.
[152] Y.H. Wang, W. Yin, W.D. Ke, W.J. Chen, C.X. He, Z.S. Ge, Biomacromolecules 19 (2018) 1990.
[153] M.F. Huo, L.Y. Wang, Y. Chen, J.L. Shi, Nat. Commun. 8 (2017) 12.
[154] P. Hu, T. Wu, W.P. Fan, L. Chen, Y.Y. Liu, D.L. Ni, W.B. Bu, J.L. Shi, Biomaterials 141 (2017) 86.
[155] D.S. Lidke, P. Nagy, R. Heintzmann, D.J. Arndt-Jovin, J.N. Post, H.E. Grecco, E.A. Jares-Erijman, T.M. Jovin, Nat. Biotechnol. 22 (2004) 198.
[156] X.H. Gao, Y.Y. Cui, R.M. Levenson, L.W.K. Chung, S.M. Nie, Nat. Biotechnol. 22 (2004) 969.
[157] K. Welsher, Z. Liu, S.P. Sherlock, J.T. Robinson, Z. Chen, D. Daranciang, H.J. Dai, Nat. Nanotechnol. 4 (2009) 773.
[158] P. Rai, S. Mallidi, X. Zheng, R. Rahmanzadeh, Y. Mir, S. Elrington, A. Khurshid, T. Hasan, Adv. Drug Deliver. Rev. 62 (2010) 1094.
[159] M.B. Zheng, C.X. Yue, Y.F. Ma, P. Gong, P.F. Zhao, C.F. Zheng, Z.H. Sheng, P.F. Zhang, Z.H. Wang, L.T. Cai, ACS Nano 7 (2013) 2056.
[160] H.Y. Cheng, D. Huo, C.L. Zhu, S. Shen, W.X. Wang, H.X. Li, Z.H. Zhu, Y.N. Xia, Biomaterials 178 (2018) 517.
[161] C. Zhang, K.L. Zhao, W.B. Bu, D.L. Ni, Y.Y. Liu, J.W. Feng, J.L. Shi, Angew. Chem. Int. Ed. 54 (2015) 1770.
[162] M.R. Horsman, J. Overgaard, Clin. Oncol. UK 19 (2007) 418.
[163] G.S. Song, C. Liang, H. Gong, M.F. Li, X.C. Zheng, L. Cheng, K. Yang, X.Q. Jiang, Z. Liu, Adv. Mater. 27 (2015) 6110.
[164] Y.H. Wang, H.G. Wang, D.P. Liu, S.Y. Song, X. Wang, H.J. Zhang, Biomaterials 34 (2013) 7715.
[165] B. Tian, C. Wang, S. Zhang, L.Z. Feng, Z. Liu, ACS Nano 5 (2011) 7000.
[166] L.R. Guo, D.D. Yan, D.F. Yang, Y.J. Li, X.D. Wang, O. Zalewski, B.F. Yan, W. Lu, ACS Nano 8 (2014) 5670.
[167] C.M.J. Hu, L. Zhang, S. Aryal, C. Cheung, R.H. Fang, L.F. Zhang, Proc. Natl. Acad. Sci. U. S. A. 108 (2011) 10980.
[168] J.-G. Piao, L. Wang, F. Gao, Y.-Z. You, Y. Xiong, L. Yang, ACS Nano 8 (2014) 10414.
[169] H. Cao, Z. Dan, X. He, Z. Zhang, H. Yu, Q. Yin, Y. Li, ACS Nano 10 (2016) 7738.

Yanmin Ju got her BS degree in Veterinary Medicine in 2014 from Nanjing Agricultural University (China). She is now in her last year as a PhD candidate at Peking University. She is interested in the biomedicine application of magnetic nanoparticles.

Dr. Bing Dong obtained his PhD in school of chemistry and molecular engineering from the East China Normal University in 2016. After postdoctoral training in department of materials science and engineering (Peking University, China), he joined the institute of magnetic materials at Hangzhou Dianzi University to develop application of two dimensional nanomaterials for microwave adsorption.

Dr. Jing Yu received her PhD degree in Advanced Materials and Mechanics from Peking University in 2015. She is now a professor in College of Materials Science and Engineering, Zhejiang University of Technology. Her current research focuses on the synthesis and biomedical applications of inorganic nanoparticles in cancer theranostics.

Yanglong Hou received his Ph. D. degree in materials science from Harbin Institute of Technology (China) in 2000. After a short post-doctoral training at Peking University, he worked at the University of Tokyo from 2002 to 2005 as a JSPS foreign special researcher and also at Brown University from 2005 to 2007 as a postdoctoral researcher. He joined Peking University in 2007, and now is a Chang Jiang Chair Professor of Materials Science. His research interests include the design and chemical synthesis of functional nanoparticles for biomedicine and energy.